JCTC Journal of Chemical Theory and Computation

pubs.acs.org/JCTC Article

Density Functional Geometries and Zero-Point Energies in Ab Initio Thermochemical Treatments of Compounds with First-Row Atoms (H, C, N, O, F)

Dirk Bakowies* and O. Anatole von Lilienfeld

Cite This: J. Chem. Theory Comput. 2021, 17, 4872−4890

Read Online

ACCESS | Metrics & More | Article Recommendations | Supporting Information

ABSTRACT: Density functionals are often used in ab initio thermochemistry to provide optimized geometries for single-point evaluations at a high level and to supply estimates of anharmonic zero-point energies (ZPEs). Their use is motivated by relatively high accuracy at a modest computational expense, but a thorough assessment of geometry-related error seems to be lacking. We have benchmarked 53 density functionals, focusing on approximations of the first four rungs and on relatively small basis sets for computational efficiency. Optimized geometries of 279 neutral first-row molecules (H, C, N, O, F) are judged by energy penalties relative to the best available geometries, using the composite model ATOMIC/B_5 as energy probe. Only hybrid functionals provide good accuracy with root-mean-square errors around 0.1 kcal/mol and maximum errors below 1.0 kcal/mol, but not all of them do. Conspicuously, first-generation hybrids with few or no empirical parameters tend to perform better than highly parameterized ones. A number of them show good accuracy already with small basis sets (6-31G(d), 6-311G(d)). As is standard practice, anharmonic ZPEs are estimated from scaled harmonic values. Statistics of the latter show less performance variation among functionals than observed for geometry-related error, but they also indicate that ZPE error will generally dominate. We have selected PBE0-D3/6-311G(d) for the next version of the ATOMIC protocol (ATOMIC-2) and studied it in more detail. Empirical expressions have been calibrated to estimate bias corrections and 95% uncertainty intervals for both geometry-related error and scaled ZPEs.

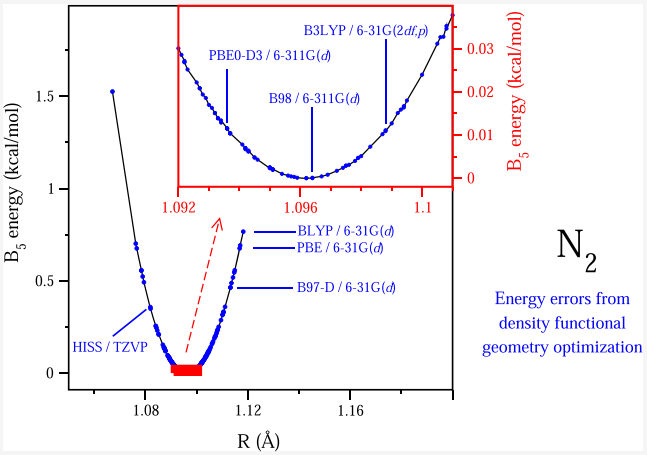

1. INTRODUCTION

Thermochemistry is a showpiece application of ab initio quantum chemistry: The reliable calculation of atomization energies provides access to experimentally relevant enthalpies of formation, but it is computationally demanding and requires accurate treatments of electron correlation. Wave function-based quantum chemistry may not meet this goal at low levels; however, it offers a clear path to converge toward the one- and *N*-particle limits of the exact solution of the electronic Schrödinger equation. Typically, only moderate effort is necessary to achieve chemically useful accuracy (~±1 kcal/mol), in particular if limited empiricism is accepted with the addition of calibrated "high-level corrections". The success of a range of popular thermochemistry protocols including Gaussian[1−4] and CBS[5] is impressive confirmation of this appraisal.

Solving the electronic problem for a given geometry is only part of the solution, however. It has long been recognized that the use of accurate geometries and the reliable estimate of anharmonic zero-point energies (ZPEs) is equally important and often poses the more taxing problem.[6,7] Early variants of the aforementioned protocols have relied on small basis set Hartree−Fock (HF) and/or MP2[8] calculations to optimize geometries and evaluate harmonic ZPEs,[1−3,5] which are then scaled to mitigate the effects of both model error and lack of anharmonic corrections. The introduction of hybrid density functional theory into the repertoire of quantum chemistry[9,10] has soon triggered attempts[11−13] to replace low-order wave function theory by B3LYP.[10,14] Nowadays, several midlevel and even some advanced thermochemistry approaches use B3LYP with basis sets of valence double- to triple-ζ quality for this purpose, including CBS-QB3[15] (6-311G(d,p)[16]), Gaussian-4[4] (6-31G(2df,p)[17]), ccCA[18] (6-31G(d)[19]), W1,[20] W3.2lite,[21] and a range of other W*n* variants[7] (cc-pVTZ[22] for molecules with first-row atoms).

Received: May 13, 2021
Published: July 14, 2021

https://doi.org/10.1021/acs.jctc.1c00474
J. Chem. Theory Comput. 2021, 17, 4872−4890

Table 1. Density Functionals Assessed in This Work[a]

rung	type	functionals used
1	LDA	SVWN3[47,48]
2	GA[b]	BLYP,[49,50] BVP86,[48,49,51] HCTH/407,[52,53] N12,[61] PBE,[54] SOGGA11[55]
	(with disp.)[c]	B97-D,[56] B97-D3(BJ)[56,57]
3	meta-GA[b]	M06-L,[58] M11-L,[59] TPSS,[62] VSXC,[63] MN12-L[60]
4	hybrid[d]	APF,[64] B1B95,[65] B1LYP,[66] B3LYP,[10,14] B3P86,[10,51] B3PW91,[10]
		B97-1,[52] B97-2,[67] ωB97,[68] ωB97X,[68] B98[70] (fit 2c), BHandH,[71,72]
		BHandHLYP,[71,72] BMK,[23] CAM-B3LYP,[73] τ-HCTHhyb,[74] HISS,[75,76]
		HSE06,[77−79] LC-ωPBE,[80] M05,[81] M05-2X,[82] M06,[83] M06-2X,[83]
		M06-HF,[84] M11,[85] MN12-SX,[86] mPW1LYP,[50,87] mPW1PBE,[54,87]
		mPW1PW91,[87,88] mPW3PBE,[54,87] N12-SX,[86] PBE0,[42−44]
		PBEh1PBE,[89] SOGGA11-X,[90] TPSSh,[91] X3LYP[92]
	(with disp.)[c]	APF-D,[64] ωB97X-D,[69] PBE0-D3[42−45]

[a]Each of the 53 functionals has been paired with basis sets 6-31G(d), 6-311G(d), and TZVP; additional basis sets have been considered for select functionals; see text. [b]GA: gradient approximation, comprising both the standard generalized gradient approximation (GGA) and a nonseparable gradient approximation (NGA).[61] [c]With dispersion correction added. [d]Collectively including any type of hybrid functional based on GGA, NGA, meta-GGA, or meta-NGA with a certain amount of either global or range-dependent exact exchange.

Other density functionals find less use in ab initio thermochemistry, one example being BMK[23] in both the G4(MP2)-6X[24] and G4(MP2)-XK[25] protocols. The bias toward B3LYP certainly reflects its unabated popularity and the proven success of the above-mentioned thermochemistry protocols, but it may also relate to the relative paucity and limited scope of density functional assessments for geometry optimizations. Most large-scale benchmarks instead focus on energetic quantities,[26−28] targeting applications that are of primary interest to density functional theory. Geometry performance has been studied in some detail by Riley et al.[29] and more recently by Brémond et al.;[30] the latter study in particular confirms the expectation that the best functionals for energetic properties are generally the most reliable ones for geometry optimizations.

Just collecting statistics about errors in geometrical parameters does not yet tell how well a functional performs in providing a reference geometry for wave function-based thermochemistry. The actual quantity of interest is the energy penalty relating to the error in geometry. Assessments of this quantity are implicit in several papers proposing revised geometry optimization protocols in thermochemistry[11,12,20] and have been reported for low-cost procedures in thermochemistry;[31] however, the number of comparisons has generally been quite limited. Vuckovic and Burke have extended the idea and proposed an analysis framework that uses the energy penalty (termed "geometry energy offset" and winkingly abbreviated to "GEO") not only to rank density functionals for accuracy but also to gain qualitative insight into geometry-related errors.[32]

Here, we present a comprehensive assessment of inexpensive density functional approaches to optimize geometries and evaluate ZPEs for ab initio thermochemistry. We use composite model B_S[33] of ATOMIC[34−36] as an accurate probe to assess energy penalties of 53 density functionals with various basis sets for a benchmark set of 279 neutral, closed-shell molecules composed of H, C, N, O, and F atoms (Section 3). Considering a wide variety of method/basis set combinations not only extends the basis for meaningful assessment, it also obviates the need for explicit and expensive geometry optimizations at the reference level of theory, as explained and demonstrated in Section 3.1. ZPEs are assessed for a subset of 50 molecules, for which accurate reference data are available (Section 4), providing both optimized scale factors and error statistics for scaled ZPEs. Recommendations are based on a combined analysis of geometry-related and ZPE errors (Section 5).

The present study is motivated by continued efforts to update the ATOMIC protocol[37,38] and make it fit for routine and inexpensive, yet reliable applications to thermochemistry. The protocol avoids empirical parametrization and implements Pople's concept of bond separation reactions[39,40] in an ab initio manner to achieve high accuracy with computationally efficient composite models (such as the aforementioned B_S). The use of (RI[41]-)MP2[8](fc)/cc-pVTZ[22] for geometry optimizations and subsequent force constant analyses remains the computational bottleneck in most calculations, warranting its replacement by more economical alternatives that promise equal or better accuracy.

PBE0-D3[42−45]/6-311G(d),[16] the method ultimately selected for use in ATOMIC-2 (to be published), is analyzed in more detail (Section 6), and simple estimates are derived and tested for both bias and uncertainty due to geometry-related and ZPE error (Sections 6.2−6.4). Section 7 summarizes our findings.

2. DETAILS OF THE STUDY

2.1. Methods Assessed. A total of 53 different first- to fourth-rung[46] density functionals[10,14,23,42−45,47−92] (Table 1) have been assessed with polarized split-valence double- and triple-ζ basis sets (6-31G(d),[19] 6-311G(d),[16] TZVP[93]). A range of other basis sets (Pople basis sets 3-21G,[94] 6-31G, and 6-311G, augmented with various sets of polarization and diffuse functions;[16,17,19,95] Ahlrichs basis sets SVP,[96] QZVP,[97] def2TZV, and def2TZVP;[98] polarization-consistent basis sets pc1 and pc2;[99] correlation-consistent basis set cc-pVTZ[22]) have been tested for some popular functionals and those that appeared particularly attractive for further consideration. HF and frozen-core MP2 (each with 6-31G(d) and cc-pVTZ basis sets) as well as MP2(full)/6-31G(d) have been added for comparison, because they have been used in thermochemical protocols in the past (Gaussian-1 to -3,[1−3] ATOMIC[34,36,37]). However, the goal is to identify a robust and, at the same time, economical geometry optimization protocol. We have thus not considered any double-hybrid functionals, which feature second-order correlation terms like MP2 and so do not offer any computational (speed) advantage over the latter. In total,

https://doi.org/10.1021/acs.jctc.1c00474
J. Chem. Theory Comput. 2021, 17, 4872−4890

we have included 219 "methods", i.e., combinations of functionals or wave function models and basis sets (see Table S1).

2.2. Benchmark Set of Molecules. The benchmark set has been assembled from earlier work[34,35,38,100] and augmented with a number of azides, small heterocycles, and other systems. Specifically, it includes the 73 molecules of the original ATOMIC paper[34] supplemented by all 26 uncharged prototypes ("parent molecules") involved in their bond separation reaction, the 173 molecules considered in the following assessment with experimental data,[35] and the 87 hydrocarbons considered recently in the development of ATOMIC(hc).[37] We have discarded duplicates, but added 28 further molecules, including 4 azides (hydrogen-, fluoro-, formyl azide and carbonyl diazide), 5 molecules identified in the "mindless" DFT benchmark of Korth and Grimme,[100] which aims at large diversity (2-azapropene, vinylamine, methanimine-*N*-oxide, methylaminomethylene, 2*H*-azirine from MB08-ORG # 1, 24, 34, 62, 70, discarding any bound molecular hydrogen), 5 heterocycles (isoxazole, oxazirine, oxazole, 1*H*-tetrazole, 1,2,3-trioxolane), 4 other molecules with structural features not considered before (formaldoxime, guanidine, hydrogen trioxide, *trans*-triazene), and 10 fluoro derivatives of molecules already included (5 FCNO isomers, *cis*-*N*-fluoroformamide, *cis*- and *trans*-nitrosyl hypofluorite, nitrogen fluoride hypofluorite, trifluoramine oxide).

In total, the benchmark includes 279 molecules (Table S2), all of which are neutral, composed of H, C, N, O, and F atoms, and treated as closed-shell species. The benchmark is not only diverse but intentionally includes "difficult" molecules such as highly strained species (e.g., tetrahedrane, cubane, oxazirines), multireference cases (e.g., ozone), unusual structures (e.g., bicyclo[1.1.0]but-1(3)-ene[37]), molecules known to cause problems for certain density functionals (e.g., nitrosyl hypofluorite,[101,102] oxirene[103,104]), and larger molecules up to the size of anthracene where small geometry errors may accumulate in their effect on evaluated single-point energies.

2.3. Computational Aspects. Density functional geometry optimizations have been performed with Gaussian09,[105] using tight SCF and geometry optimization criteria (keywords "SCF = Tight" and "Opt = Tight" in Gaussian, largest observed root-mean-square (RMS) force: 1.3×10^{-5} au) and "ultrafine" pruned integration grids. Subsequent force constant calculations have identified optimized structures as true minima in 98.6% of all 61 101 (219 methods, 279 molecules) cases. Most of the remaining 862 optimizations involve molecules with extremely flat potential energy surfaces of essentially barrier-free rotation or pseudorotation such as 2-butyne (36 methods affording imaginary frequencies), cyclopentane (208), and 2,4-hexadiyne (176), and in fact, imaginary frequencies remain below 30*i* cm^{-1} in 60% of all cases. Genuine transition states have been recorded for a few molecules, including for planar naphthalene and anthracene (at the MP2/6-31G(d) level) and for oxirene (for 116 out of 219 methods); both problem cases are well documented in the literature.[103,104,106] We have not attempted to resolve any of these cases with imaginary frequencies and simply report their number for each of the 219 methods tested (Table S1). Note, however, that no imaginary frequencies have been recorded for the subset of 50 molecules included in the zero-point energy benchmark (Section 4). For a different subset of 99 smaller molecules, geometries have also been optimized at the CCSD(T)[107−109]/cc-pVTZ[22] level using the CFOUR[110] package. Subsequent force constant analyses have identified all optimized geometries as true minima.

Geometries are probed with ATOMIC composite model B_5,[33,36] and some validation is performed with the more advanced model A,[33,34] both of which involve correlated wave function calculations using standard correlation-consistent basis sets[111−113] (cc-pV*X*Z,[22,114] cc-pCV*X*Z[115]). MOLPRO[116,117] has been used for all CCSD and CCSD(T) and some MP2 single-point energies; however, most MP2 calculations have been run with TURBOMOLE[118,119] (versions 6.2, 7.1) using the RI approximation[120] for computational efficiency and large auxiliary basis sets[121,122] for accuracy (cc-pV(*X*+2)Z, cc-pwCV(*X*+2)Z for atomic cc-pV*X*Z and cc-pCV*X*Z basis sets).

3. GEOMETRIES

For the purpose of this paper, it is neither necessary nor particularly productive to examine geometrical parameters in much detail. The objective is to identify an optimization protocol that minimizes the adverse effect of geometrical error on high-level single-point energies, and statistics on bond length and angle errors do not provide all of the necessary information. The functional relation between energy and geometrical displacement can be well approximated by harmonic (quadratic) force fields, showing that individual geometric errors can have a large impact only if the associated force constant is large and that many smaller errors may be more tolerable than few larger ones.

We use the ATOMIC/B_5 energy as a probe to judge the quality of a particular geometry. B_5 is among the most attractive composite models that approximates the complete basis set limit of all-electron CCSD(T) at a low cost.[36] It is quite successful in reproducing very high-level bond separation energies[36,38] and can therefore be expected to fare well also for energy differences of small geometric displacements (see Section 3.1).

The use of an energy criterion even obviates the need for external reference data to compare to. Knowing that the lowest energy will be obtained for a geometry fully optimized at that level, we can identify the method, i.e., the combination of wave function or density functional and basis set, that provides the best approximation to that geometry. We simply compare B_5 single-point energies for all 219 geometries generated for a molecule and identify the "best" geometry as the one showing the lowest B_5 energy overall. This works of course only if all geometry optimizations lead to stationary points, in each case properly associated with the corresponding structure of a particular molecule. We have identified only one problem case among all 61 101 optimizations (oxazirine rearranging to isocyanic acid, HNCO, at the HF/6-31G(d) level) and have removed that one from all further analysis.

The procedure may be regarded as an incomplete geometry optimization at the B_5 level that uses auxiliary trial structures from lower-level approaches at no additional cost instead of generating increasingly refined geometries using expensive gradient information. We have augmented the set of trial structures with highly accurate model A geometries obtained previously for 27 hydrocarbons[38] and additional CCSD(T)/cc-pVTZ geometries (obtained here with CFOUR[123]) for 99 smaller molecules of the benchmark. The final collection of lowest B_5 energies for each of the 279 molecules forms the database that we use to assess each of the individual 219 methods.

https://doi.org/10.1021/acs.jctc.1c00474
J. Chem. Theory Comput. 2021, 17, 4872−4890

Using nomenclature compatible with previous ATOMIC papers,[34,37,38] we may formally define geometry-related error as the energy penalty arising from using an approximate equilibrium ("e") geometry $\tilde{G}_e^k$ that was optimized for molecule M with a method labeled k

$$\Delta E_e^{\mathrm{geo},k}[M] = E^{\mathrm{exact}}[M;\, \tilde{G}_e^k[M]] - E^{\mathrm{exact}}[M;\, G_e^{\mathrm{exact}}[M]] \tag{1}$$

and then introduce a series of approximations to illustrate our approach; first, the replacement of the exact energy E^{exact} by that of a suitably chosen composite model m (here: B_5), second, the replacement of the exact equilibrium geometry $G_e^{\mathrm{exact}}[M]$ by that optimized with composite model m, and finally, the approximation of the latter by the best available approximate equilibrium geometry $\tilde{G}_e^{k_{\mathrm{opt}}}[M]$, i.e., the one optimized with the particular method $k = k_{\mathrm{opt}}$ that minimizes $E^{\{m\}}[M;\, \tilde{G}_e^k[M]]$

$$\begin{aligned}\Delta E_e^{\mathrm{geo},k}[M] &\approx E^{\{m\}}[M;\, \tilde{G}_e^k[M]] - E^{\{m\}}[M;\, G_e^{\mathrm{exact}}[M]] \\ &\approx E^{\{m\}}[M;\, \tilde{G}_e^k[M]] - E^{\{m\}}[M;\, G_e^{\{m\}}[M]] \\ &\approx E^{\{m\}}[M;\, \tilde{G}_e^k[M]] - E^{\{m\}}[M;\, \tilde{G}_e^{k_{\mathrm{opt}}}[M]]\end{aligned} \tag{2}$$

In Section 6.2, we shall analyze errors for the finally selected geometry optimization method (index k henceforth dropped) and calibrate a model to estimate a bias correction $C_{\mathrm{A,e}}^{\mathrm{geo}}[M]$ that annihilates the error $\Delta E_{\mathrm{A,e}}^{\mathrm{geo}}[M]$ in atomization energy *on average* (note that $\Delta E_{\mathrm{A,e}}^{\mathrm{geo}}[M] = -\Delta E_e^{\mathrm{geo}}[M]$), as well as a corresponding uncertainty $u_{\mathrm{A,e}}^{\mathrm{geo}}[M]$ for molecule M such that

$$|C_{\mathrm{A,e}}^{\mathrm{geo}}[M] + \Delta E_{\mathrm{A,e}}^{\mathrm{geo}}[M]| \le |u_{\mathrm{A,e}}^{\mathrm{geo}}[M]| \tag{3}$$

is fulfilled with high confidence (95% or better for a balanced test set $M \in \{M_1, M_2, \ldots\}$).

3.1. Assessment of the Analysis Procedure. Figure 1 shows results in the form of a heat map. One pixel each is drawn for the combination of a method (abscissa) and a molecule (ordinate), indicating the error in B_5 energy relative to the method identified as best for that molecule. A logarithmic energy scale has been chosen intentionally that distinguishes between "optimal" (black or dark green, <0.005 kcal/mol), near-optimal (any shade of green, <0.05 kcal/mol), and potentially problematic (very pale green or white, >0.05 kcal/mol). Data points representing the "best" method for a particular molecule have arbitrarily been assigned a value of 0.001 kcal/mol to ensure they fit the logarithmic energy scale.

Molecules have been sorted from difficult (bottom) to simple (top) and methods from inaccurate (left) to accurate (right), taking root-mean-square deviations over all methods and all molecules, respectively, as sorting criteria. Individual methods and molecules may be identified by their indices listed in Tables S1 and S2.

Results for external reference methods (model A, CCSD(T)/cc-pVTZ) are displayed on the very right, using longer bars instead of individual pixels. Recall that data are available only for limited subsets of molecules (s.a.), so here many uncolored or white stretches (all in the case of model A) refer to missing data rather than significant energy error.

Inspection of Figure 1 and of corresponding raw data (Table S1) allows a number of conclusions to be drawn: There is no single method that excels for all molecules. Each method shows in fact at least one error larger than 0.4 kcal/mol. On the other hand, 85 out of 219 methods contribute at least 1 "best hit", 44 contribute more than 1, and 3 of them contribute more than 15 each (see top bar of Figure 1). In some cases, best hits may be landed by chance: B97-2/6-31G(d), for example, provides the best geometry for oxirene, although it turns out to be a transition state at that level (C−O, 1.489 Å, C═C, 1.266 Å, C−H 1.073 Å; compare CCSD(T)(fc)/aug′-cc-pV6Z:[124] 1.496, 1.270, 1.069 Å). Even a number of those methods that disappoint overall (left-hand side of Figure 1) contribute some "best geometries" or at least geometries that are very close to optimal (dark spots in Figure 1). Obviously, every method has its own strengths and weaknesses and the B_5-energy criterion lets us identify the strengths and provide information that we use to build up the reference database.

Of course, only explicit geometry optimization at the B_5 level could quantify the reliability of this database. Prohibitive computational expense forced us to discard this idea, but the analysis of limited external reference data certainly helps:

The first external reference, CCSD(T)/cc-pVTZ, is generally regarded to be quite accurate for geometries, and a root-mean-square deviation (RMSD) of 0.0036 Å relative to the basis set limit has been reported for 138 unique bond lengths of first-row molecules.[124] Still we do not observe a single best hit from any of the 99 CCSD(T)/cc-pVTZ geometry optimizations performed here (Tables S1 and S2). This may surprise at first glance, but one needs to keep in mind that the applied energy probe (model B_5) is significantly more advanced than CCSD(T)/cc-pVTZ, as it approximates the complete basis set limit of all-electron CCSD(T) through extrapolation of frozen-core MP2 energies, augmented with smaller basis set evaluations of CCSD, (T), and core-correlation increments. Recently Warden et al. have proposed a related focal-point approximation for frozen-core CCSD(T) geometry optimizations[125] that likewise combines CBS estimates of MP2 with smaller basis set evaluations of the difference between CCSD(T) and MP2 and is demonstrated to reproduce large basis set CCSD(T) geometries with high accuracy. In summary, we may conclude that the collection of "best methods" provides more accurate geometries than CCSD(T)/cc-pVTZ for any of the 99 molecules tested. Statistical assessment further indicates a tendency of CCSD(T)/cc-pVTZ to overestimate bond lengths slightly (compared to "best geometries", 359 bonds: mean signed error (MSE) = 0.006 Å, mean unsigned error (MUE) = 0.008 Å, data not shown in detail), which is in qualitative agreement with observations reported by Spackman et al.[124]

The second external reference (model A, 27 geometries taken from earlier work[38]) contributes 17 "best hits" to our database and shows energy penalties of less than 0.01 kcal/mol in all remaining 10 cases (Table S2). This demonstrates the close agreement of model B_5 with model A, which is an alternative, more accurate, approximation to all-electron CCSD(T)/CBS. One may ask how well our procedure would work in the absence of model A geometries: For 16 out of the 17 "best hit" cases, there is at least one method in the pool of 219 that has an energy penalty of less than 0.05 kcal/mol; in only one case, we observe larger but still acceptable 0.10 kcal/mol (MN12-L/TZVP, bicyclo[1.1.0]-but-1(3)-ene; data not shown in detail).

In summary, we can expect that our choice of "best" geometries as reference introduces energy errors of less than 0.1 kcal/mol in most cases, and typically much less than this.

https://doi.org/10.1021/acs.jctc.1c00474
J. Chem. Theory Comput. 2021, 17, 4872−4890

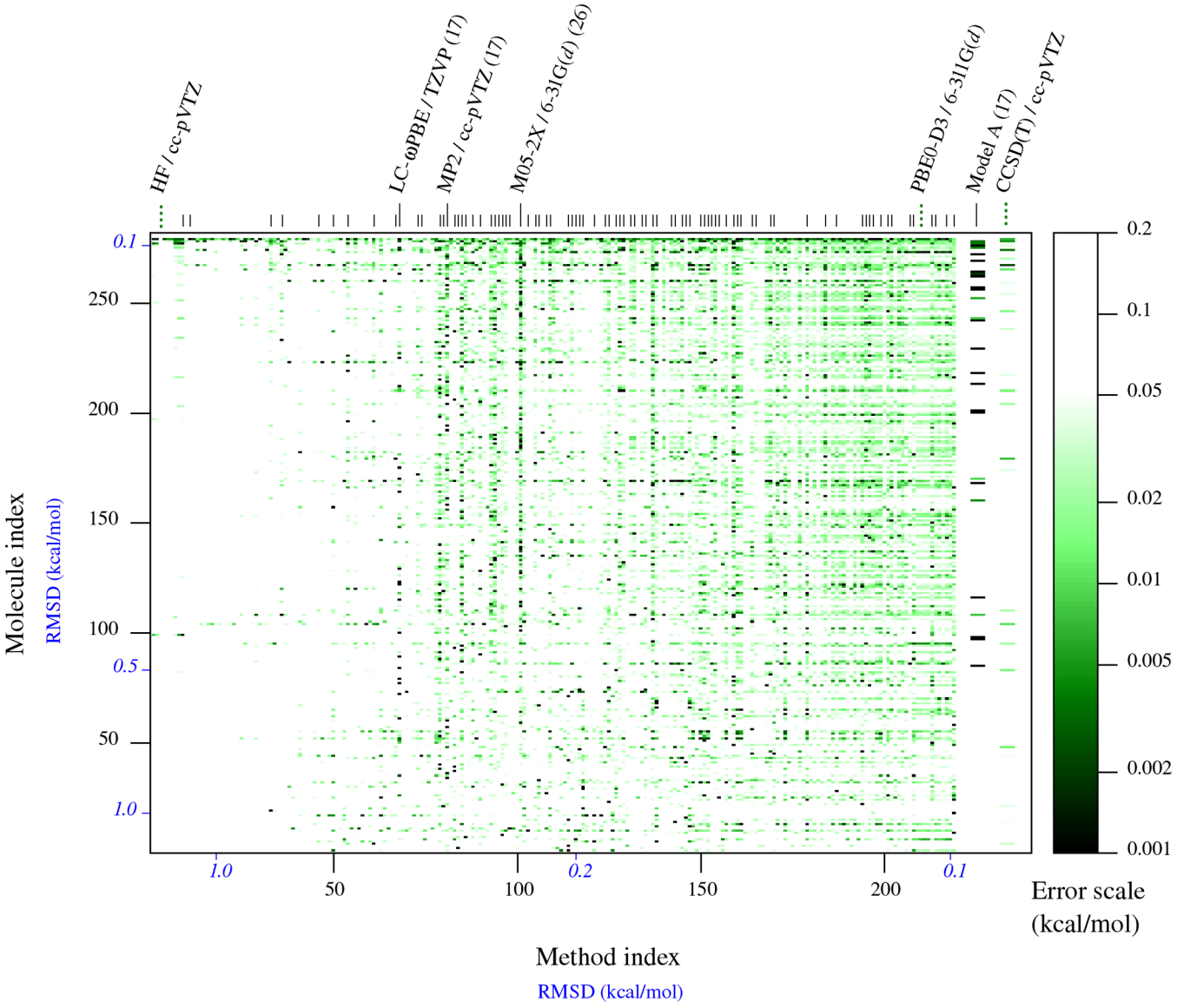

Figure 1. Heat map showing the error in B_5 energy observed for a given molecule (ordinate) using geometries optimized with a given method (abscissa). Molecules have been sorted for RMS deviations over all methods, and methods have likewise been sorted for RMS deviations over all molecules. See Tables S1 and S2 to identify methods and molecules by their index. RMS deviations for select methods and molecules are indicated in blue italic style. Methods contributing a "best" geometry are indicated on the top bar, those with more than 15 "best" hits and select others are named explicitly. See text for more details.

3.2. Performance of Individual Methods. Individual methods show RMS energy penalties relative to this reference that vary between excellent 0.09 kcal/mol (B1B95/6-31+G(d)) and unacceptable 2.12 kcal/mol (HSE06/3-21G, see Table S1). A majority of 55% of all methods show reasonable values of 0.25 kcal/mol or less. Figure 2 provides a histogram-style overview of RMS and maximum error statistics, pooling methods of a particular density functional approximation and basis set (view limited to 6-31G(d), black; 6-311G(d), red; TZVP, blue).

LDA and GGA functionals perform quite poorly overall, never reaching RMS errors below 0.4 kcal/mol. Somewhat surprisingly SVWN3 still performs better (0.6 kcal/mol) than either BLYP (1.5) or BVP86 (0.9) if combined with a triple-ζ split-valence basis set. The nonseparable gradient approximation of N12 is more successful but does not fully convince either (RMS ∼ 0.3 kcal/mol).

The best-performing nonhybrid functionals go beyond the generalized (or nonseparable) gradient approximation and reach RMS errors down to 0.2 kcal/mol (MN12-L with split-valence double- or triple-ζ basis set). Hybrid approximations are required to push numbers further down to 0.1 kcal/mol, but they are not a guarantee of good performance: Among different hybrid functionals, RMS errors still vary by up to an order of magnitude (Figure 2, bottom panel), so do maximum errors (top panel). This observation sounds a note of caution to select functionals carefully and check all statistical parameters; a particular method may be performing well on average but not be robust enough for general use, if significant problems are observed for a few molecules.

Fortunately, the simple polarized split-valence double-ζ basis set (6-31G(d)) behaves quite well in general, and some hybrid functionals (notably, B1B95 and mPW1PW91, Table S1) paired with it show excellent performance not far from the

https://doi.org/10.1021/acs.jctc.1c00474
J. Chem. Theory Comput. 2021, 17, 4872−4890

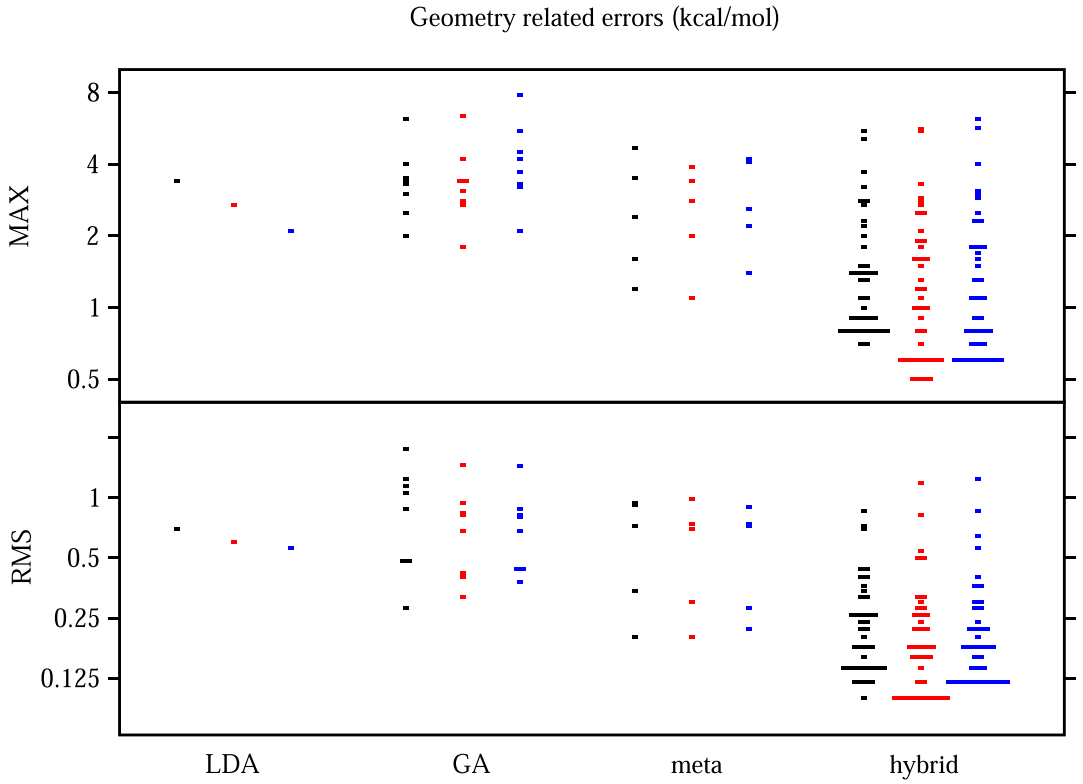

Figure 2. Geometry errors assessed by ATOMIC model B_5 as energy probe. The top panel shows maximum observed errors, and the bottom panel shows RMS errors, each evaluated for the complete set of 279 molecules. Assessed density functionals are not specified individually but classified by type (1 LDA, 8 GA (GGA/NGA), 5 meta (meta-GGA, meta-NGA), 39 hybrid), and colors indicate the basis set used (black, 6-31G(d); red, 6-311G(d); blue, TZVP). Data are shown as histograms; bars are drawn with a vertical resolution of 0.1 kcal/mol (top) and 0.02 kcal/mol (bottom), and their length is chosen proportional to the number of functionals representing a particular value. A logarithmic scale has been chosen for improved clarity.

overall best result of 0.09 kcal/mol. Extension to polarized split-valence triple-ζ (6-311G(d)) often improves results. The addition of further valence, polarization, or diffuse functions has only been studied for a few functionals; it helps in some cases (e.g., B3LYP, Table S1 in agreement with earlier observations[126]), but has a negative impact in others (compare, e.g., PBE0/6-311G(d), 0.11 kcal/mol, PBE0/QZVP, 0.15 kcal/mol). On the other hand, it is essential to retain polarization functions on nonhydrogen atoms; none of the otherwise successful functionals PBE0 and HSE06 achieves RMS errors below 1.5 kcal/mol if combined with unpolarized basis sets (3-21G, 6-31G, def2TZV).

4. ZERO-POINT ENERGIES

It is common practice in most thermochemistry approaches (including Gaussian-n,[1−4] ccCA,[18,127] and Weizmann-1[20]) to estimate zero-point energies (ZPEs) from scaled harmonic frequencies ω_i ($ZPE^{scal} = f_{scal}ZPE = 1/2 \cdot f_{scal} \sum_i \omega_i$). Scaling eliminates or at least reduces average biases introduced through both methodological shortcomings and the neglect of anharmonic contributions. To calibrate f_{scal}, we have resorted to a training subset of 50 molecules, for which we have previously assembled accurate anharmonic ZPEs,[38] both from experimental and theoretical sources (Table S3). The calibration follows standard protocols,[128] minimizing the squared sum of differences between reference and scaled harmonic ZPEs. Table S4 lists optimized scale factors and error statistics for all 219 methods considered here. A number of these methods have already been assessed in the past,[129−131] reported scale factors either match ours or are slightly smaller (by up to 0.005), reflecting differences in the training sets employed. We note in particular that optimized scale factors for MP2/cc-pVTZ (0.979) and B3LYP/cc-pVTZ (0.990) are very close to values recommended for use in thermochemical applications (0.98[35] and 0.989[131,132]).

4.1. Performance of Individual Methods. RMS errors of scaled ZPEs vary from 0.13 (TPSSh/TZVP) to 0.53 kcal/mol (HSE06/3-21G), spanning a much smaller 4-fold range than we have observed for geometry-related error (25-fold). This may in part reflect the use of an optimized scale factor that evens out ZPE error and the paucity of accurate reference data that seriously limits the size of the benchmark, but it also highlights the fact that geometry-related error is potentially more problematic, because it scales quadratically with displacement from a true reference geometry. The encouraging news is that 82% of all methods (179 methods, see Table S4) achieve an acceptable 0.25 kcal/mol RMS error in ZPEs, far more than observed for geometry-related errors (s.a.). Notable exceptions include HF and MP2 with various basis sets, M06-HF, a functional with 100% exact exchange, the meta-GGA M11-L, and generally choices based on unpolarized basis sets (3-21G, 6-31G, def2TZV). There is no clear-cut correlation between the level of density functional approximation and ZPE accuracy; in fact, functionals with RMS errors close to the best performer, a hybrid functional (TPSSh/TZVP, s.a.), can be found among the lowest two rungs: SVWN3/6-31G(d) (0.15 kcal/mol), N12/6-31G(d) (0.14 kcal/mol) (see Figure 3).

https://doi.org/10.1021/acs.jctc.1c00474
J. Chem. Theory Comput. 2021, 17, 4872−4890

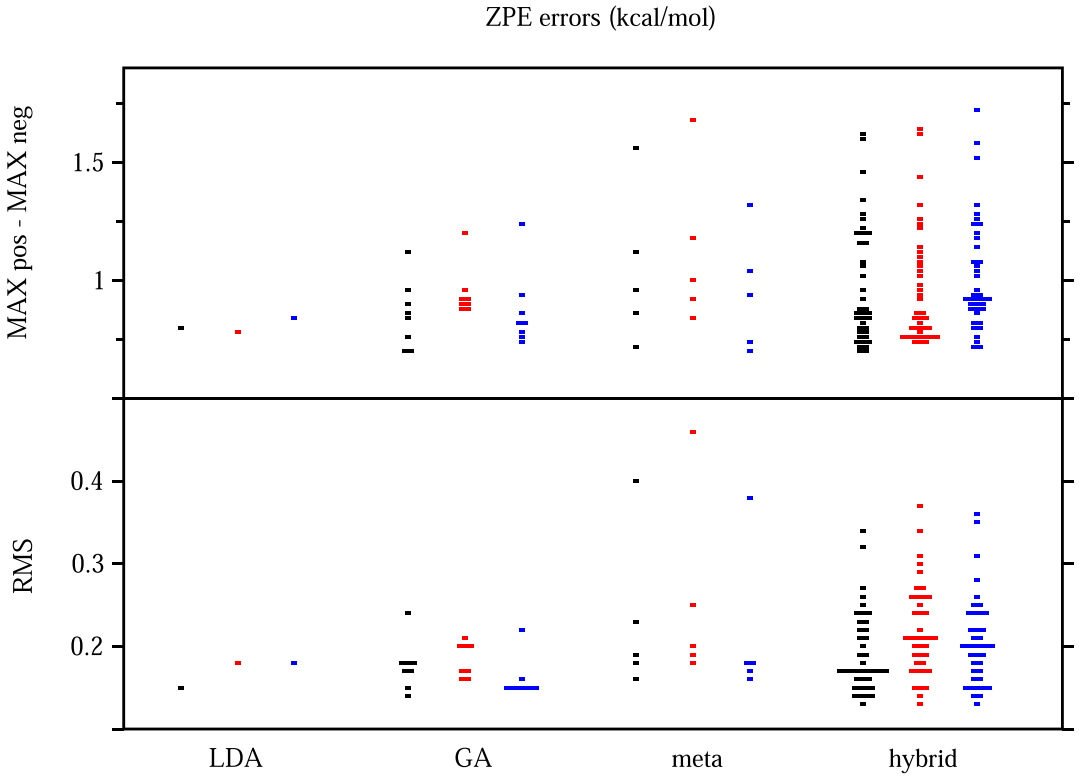

Figure 3. ZPE errors observed for the calibration set (50 molecules) after scaling. The top panel shows error ranges (differences between maximum positive and maximum negative errors), and the bottom panel shows RMS errors. Like in Figure 2, the assessed density functionals are not specified individually but classified by type (1 LDA, 8 GA (GGA/NGA), 5 meta (meta-GGA, meta-NGA), 39 hybrid), and colors indicate the basis set used (black, 6-31G(d); red, 6-311G(d); blue, TZVP). Data are shown as histograms; bars are drawn with a vertical resolution of 0.02 kcal/mol (top) and 0.01 kcal/mol (bottom), and their length is chosen proportional to the number of functionals representing a particular value.

Only double-hybrid functionals are known to have a distinct advantage;[131,133] we have tested two options just to offer a point-of-reference. Both B2-PLYP[134]/cc-pVTZ and mPW2-PLYP[135]/cc-pVTZ undercut the RMS error of TPSSh/TZVP by about one-third (Table S4). Such excellent performance requires balanced basis sets with several sets of polarization functions,[131] however, making the use of double-hybrid functionals computationally very expensive and unattractive for the purposes of our study. Moderating expectations on accuracy, there are still a number of interesting first- to fourth-rung functionals to choose from that all have relatively low RMS and maximum errors and that get by with small basis sets; see Figure 3.

5. OVERALL ASSESSMENT: GEOMETRY-RELATED AND ZPE ERRORS

Figure 4 compares geometry-related and ZPE errors for all 53 density functionals, HF, and MP2, showing results for standard small basis sets (6-31G(d), 6-311G(d), TZVP, see Figures 2 and 3) and, as far as available, also for the larger basis sets 6-31G(2df,p) and cc-pVTZ, which have found use in popular thermochemistry protocols (G4, some Weizmann variants, each with B3LYP). Approaches are sorted for the combined RMS error, i.e., the RMS of individual, geometry-related, and ZPE, RMS errors, for each approach taking the most successful basis set. The value of this metric ranges from 1.52 (HF/6-31G(d)) down to 0.30 (TPSSh/6-311G(d)) on the left-hand side of Figure 4 and from 0.28 (M06/6-31G(d)) down to 0.20 (B1B95/6-31G(d)) on the right-hand side, which besides MN12-L only includes hybrid functionals. The metric cannot serve as an absolute criterion, because geometry-related errors are assessed for a significantly larger and more diverse set of molecules, but it is still quite useful, because it identifies less-than-ideal methods (on the left-hand side) that suffer from above-average errors in at least one of the two categories, geometries, or ZPEs.

Geometry-related error is the knock-out criterion for all methods in the upper two-thirds section of the left-hand-side panel, with RMS errors regularly approaching or exceeding 0.5 kcal/mol and maximum errors often being outside the range displayed (+3 kcal/mol). Scrutiny of individual data (available in the Supporting Information) shows that molecules with high heteroatom content, generally those with small molecule index in Figure 1 and Table S2, are among the worst offenders in most cases, including tetrafluorohydrazine, perfluoroperoxide, F_2NOF, and various azides, to just name a few. *cis*-FONO is a special case causing problems for some methods that perform well otherwise (indicated by dashed lines in Figure 4; e.g., B3PW91 and mPW3PBE with 6-311G(d) basis set). It is known to have two distinct minima along the F−O stretch coordinate (at ≈1.43 and ≈1.7 Å);[136] and we must assume that our assessment, producing a nearly continuous range of F−O distances between 1.35 and 1.82 Å for 219 methods, has not always identified the lowest minimum. Some other well-performing functionals, including B1LYP, B3LYP, B97-1, B98, and τ-HCTHhyb, show weaknesses for geometries of larger saturated hydrocarbons that improve upon basis set extension (compare Figure 4). MP2 stands out with known problems for triple bonds[35] (particularly in tetracyanomethane, see Table S2), but the real surprise is BMK that is conspicuous for

https://doi.org/10.1021/acs.jctc.1c00474
J. Chem. Theory Comput. 2021, 17, 4872−4890

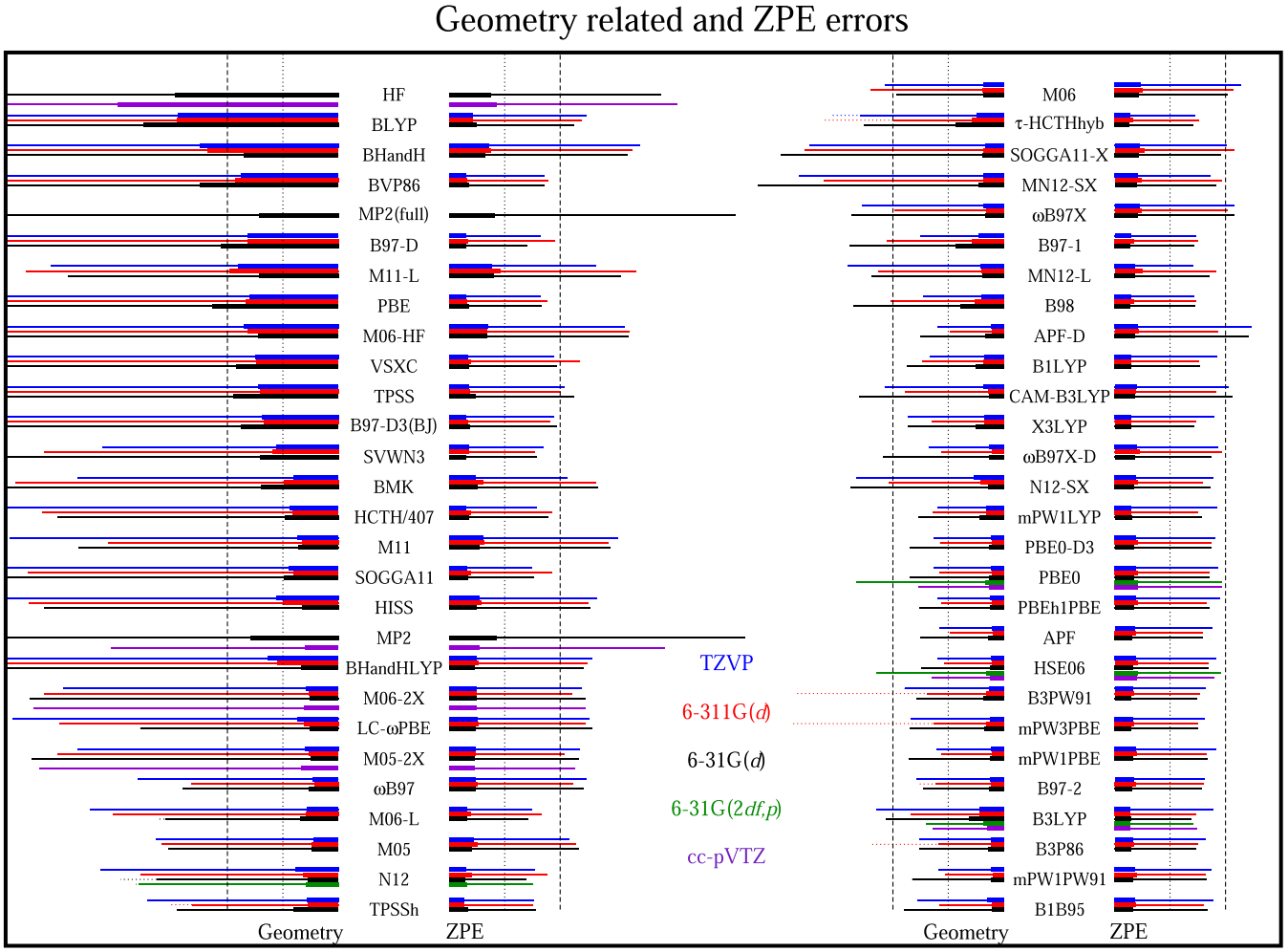

Figure 4. Geometry-related and ZPE errors for 53 density functionals, HF, and MP2 with select basis sets (color coded). Vertical dotted and dashed guide lines represent errors of 0.5 and 1.0 kcal/mol, respectively. RMS errors for 279 molecules (geometry, 278 for HF/6-31G(d), see text) or 50 molecules (ZPE) are shown as thick lines; maximum errors (geometry) and error ranges, i.e., differences between maximum positive and negative errors (ZPE) are plotted as thin lines. Error values larger than 3 kcal/mol are truncated (see left-hand side) for improved clarity. Dotted thin lines are used in those cases, in which the largest geometry error pertains to *cis*-FONO; the solid section then indicates the largest error found among all other molecules. This distinction is made because *cis*-FONO is known to have two distinct minima, and no attempt was made to locate both (see text for details). Methods are ordered from top left to bottom right, using as sorting criterion a decreasing squared sum of RMS errors for geometry and ZPE, in each case taking the most successful basis set displayed. Raw data are collected in Tables S1 and S4.

overestimating C−C bond lengths in strained hydrocarbons, e.g., in tetrahedrane ("best hit" reference 1.474 Å, BMK/6-31G(d): 1.521 Å). The situation seems to improve with basis set size (BMK/TZVP: 1.512 Å, compare also Figure 4), but we have not tested BMK/6-31+G(2df,p) and so cannot comment on the geometry optimization protocol used in G4(MP2)-6X.[24] N12/6-31G(d) has recently been suggested as promising low-cost alternative;[31] our assessment indeed shows excellent performance for ZPEs but only average quality for geometries (Figure 4).

We shall not discuss any further details on specific geometry problems but rather focus on methods that behave well for both geometry optimizations and ZPE evaluations (right-hand side of Figure 4). Using just the sorting criterion of combined RMS error, it would be easy to identify B1B95/6-31G(d) as the best candidate for a midlevel thermochemistry protocol, one that by the way uses a very small basis set and so promises high computational efficiency. In reality, however, values of the sorting criterion span such a small range for methods listed on the right-hand side that each of them can be recommended if combined with the individually most promising basis set. We note in particular that B3LYP combined with either 6-31G(2df,p) or cc-pVTZ shows excellent performance, providing support for its use in popular thermochemistry protocols (G4, several variants of Weizmann). We choose the following guiding principles to select an alternative protocol: simplicity of the functional, small basis set size, good overall performance, and avoidance of excessive maximal errors. After resolving remaining issues with imaginary frequencies (Table S1), the chosen protocol should also find a true energy minimum for each of the 279 molecules considered. The latter two conditions seem particularly important, since we wish to not only ensure good overall accuracy but also robustness in "difficult" situations. A few functionals disappoint in this respect; SOGGA11-X and MN12-SX, e.g., show excessive geometry-related error (>1.5 kcal/mol, Figure 4) for perfluoroperoxide.

5.1. Choice of an Inexpensive Method for Geometry Optimizations and ZPE Evaluations. In the end, we have selected PBE0-D3/6-311G(d), which is not only among the

https://doi.org/10.1021/acs.jctc.1c00474
J. Chem. Theory Comput. 2021, 17, 4872−4890

Table 2. Relative Energies of Alanine Tetrapeptide Conformers

level used for		conformer[a]										
single-point energy	geometry optimization	1	2	3	4	5	6	7	8	9	10	source
HF/6-31G(d,p)	HF/6-31G(d,p)	0.23	0.82	0.00	2.38	2.41	1.24	6.36	4.34	7.23	7.49	ref 137
LMP2/cc-pVTZ(-f,-d)	HF/6-31G(d,p)	2.71	2.84	0.00	4.13	3.88	2.20	5.77	4.16	6.92	6.99	ref 137
HF/6-31G(d,p)	HF/6-31G(d,p)	0.31	0.90	0.00	2.49	2.47	1.25	6.45	4.33	7.23	7.59	this work[b]
MP2/cc-pVTZ	HF/6-31G(d,p)	4.33	4.25	0.00	5.68	5.38	1.86	5.94	3.81	7.40	7.02	this work[c]
model B_5	HF/6-31G(d,p)	3.40	3.40	0.00	5.00	4.64	2.13	5.94	4.13	7.18	7.39	this work
model B_5	MP2/cc-pVTZ	4.51	4.33	0.00	5.85	5.53	2.02	6.29	4.40	7.60	7.28	this work
model B_5	PBE0-D3/6-311G(d)	4.59	4.50	0.00	5.88	5.74	2.14	6.29	4.44	7.83	7.30	this work
model B_5	PBE0/6-311G(d)	4.57	4.52	0.00	6.01	6.23	2.31	6.45	4.63	7.84	8.02	this work

[a]See ref 137 for definition of conformers. All energies are reported in kcal/mol, relative to the energy of conformer 3. [b]The results of ref 137 could only be reproduced approximately (compare above), relative energies deviating by up to 0.11 kcal/mol. We also note that some optimized ϕ and ψ angles differed by up to 9° from values reported in ref 137 (not shown in detail). We attribute these differences to the tighter convergence criteria used here for geometry optimizations (RMS gradient $<10^{-6}$ au in all cases, $<3 \times 10^{-4}$ au reported in ref 137). [c]All MP2/cc-pVTZ calculations use the RI approximation (TURBOMOLE). The large differences with respect to LMP2/cc-pVTZ(-f,-d) reported in ref 137 are likely due to our choice of not neglecting higher-angular-momentum functions and not reverting to local correlation, choices that more than 20 years ago (ref 137) would not have been feasible.

very best candidates but is attractive also for two other reasons: First, the functional is largely "ab initio" and contains calibrated parameters only in the added dispersion term. Second, and maybe even more importantly, it is widely available and implemented in almost all quantum chemistry codes that allow for density functional calculations. The addition of a dispersion term promises some advantage for larger molecules as discussed below. The basis set 6-311G(d) has been given preference because it shows excellent geometry performance for PBE0(-D3) (Table S1) and at the same time contains fewer functions than most reasonable alternatives. Overall accuracy is comparable to popular B3LYP as used in G4 and in some Weizmann variants, slightly better in geometries and a little worse in ZPEs. The distinguishing factor is that PBE0 and PBE0-D3 achieve good performance with small basis sets already (6-31G(d): 2 and 15 functions on H and C, N, O, F atoms, respectively; 6-311G(d): 3 and 18), while B3LYP needs larger basis sets to achieve that goal (6-31G(2df,p): 5 and 28; cc-pVTZ: 14 and 30; see Figure 4), translating into a very significant computational (speed) advantage of PBE0(-D3) for both geometry optimization and force constant calculation.

5.2. Dispersion Corrections. Table S2 lists individual results for select geometry optimization protocols. As expected, the dispersion term in PBE0-D3 has a negligible effect for most molecules; however, we see a small advantage for a number of larger hydrocarbons for which dispersion effects on geometries are plausible. We have selected the classic example of alanine tetrapeptide (Ac-(Ala)$_3$-NHMe, $C_{12}H_{22}N_4O_4$) as additional test case to assess the effects of dispersion terms on geometries and on accurate energies (B_5) evaluated for those geometries. More than 20 years ago Beachy et al. have optimized 10 conformers at the HF/6-31G(d,p) level and obtained local MP2 single-point energies as a benchmark for classical force fields.[137−139] More recently, Distasio et al. have optimized the geometries of two conformers (extended, #1 and globular, #3) at the MP2/cc-pVTZ level and noted significant long-range correlation effects on conformer geometries and resulting conformational energy gaps at the complete basis set limit of MP2.[140] Note that MP2 is the only tractable fully ab initio option to probe effects of long-range dispersion in larger molecules. It may not be a reliable reference for local geometric parameters such as bond lengths (Table S1), but any problems related to these should effectively cancel out in the analysis of relative (conformational) energies.

Here, we have performed geometry optimizations for all 10 conformers at the HF/6-31G(d,p), MP2/cc-pVTZ, PBE0/6-311G(d), and PBE0-D3/6-311G(d) levels. Results shown in Table 2 confirm Distasio's general observation for the entire set of conformers and at a higher level chosen for single-point energies. They further show that relative energies (B_5) computed for PBE0-D3 geometries match those computed for MP2 geometries quite well, improving on PBE0 geometries in a number of cases (particularly for conformers 4−8 and 10 relative to 3). In summary, the dispersion term in PBE0-D3 has a negligible effect on geometries of smaller molecules, but there is some evidence that it helps improve the situation for larger species.

6. ASSESSMENT OF PBE0-D3/6-311G(D)

PBE0-D3/6-311G(d) will be used in the updated version of the ATOMIC protocol (ATOMIC-2, to be published) to optimize geometries and estimate anharmonic ZPEs from scaled harmonic values (f_{scal} = 0.979, Table S4). Here, we assess this choice in more detail and calibrate simple expressions that correct for average bias in atomization energies ($C^{geo}_{A,e}[M]$) and ZPEs ($C^{ZPE}[M]$) and estimate 95% uncertainty intervals ($u^{geo}_{A,e}[M]$, $u^{ZPE}[M]$). Final results, including bias corrections and uncertainty estimates, will be referred to as ATOMIC-2$_{um}$ ("um" for uncertainty model).

6.1. Analysis of Cases with Imaginary Frequencies. Geometries optimized at the PBE0-D3/6-311G(d) level have been identified as transition states in three cases. In two of them (2,4-hexadiyne and cyclopentane), imaginary frequencies are very small (7i, 17i cm^{-1}) and careful reoptimization of slightly distorted structures affords true minima that are 8×10^{-5} kcal/mol lower and 9×10^{-5} kcal/mol higher (!) in energy, respectively. The tiny energy differences and their sign in the second case demonstrate that numerical precision may not be sufficient to determine the nature of the stationary point and that the modes corresponding to rotation (2,4-hexadiyne) and pseudorotation (cyclopentane) should rather be consid-

https://doi.org/10.1021/acs.jctc.1c00474
J. Chem. Theory Comput. 2021, 17, 4872−4890

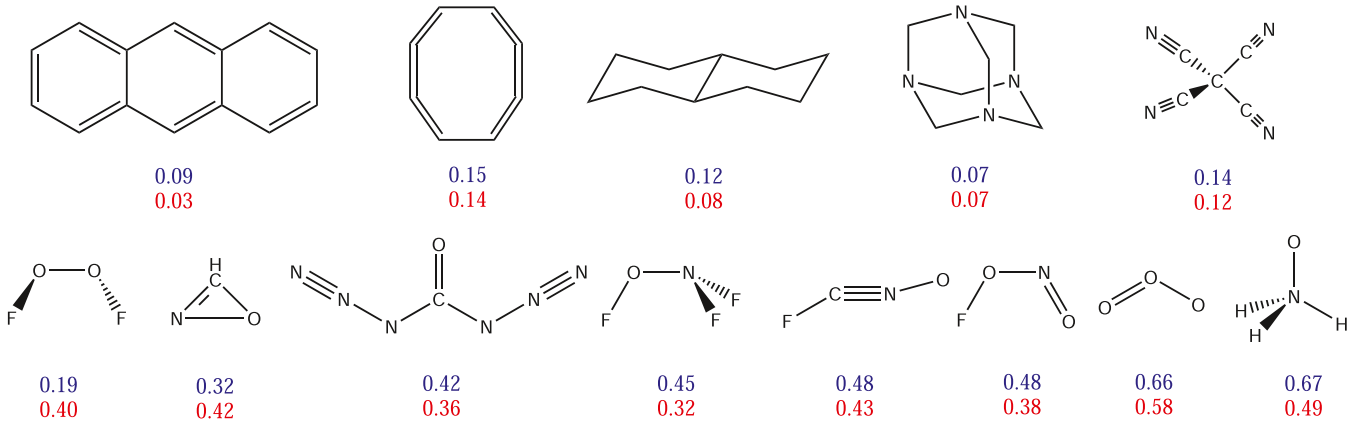

Figure 5. Energy error in kcal/mol resulting from the use of PBE0-D3/6-311G(d) geometries, evaluated with composite models A (blue) and B_5 (red) as energy probes. A few of the largest molecules in the set are shown (top) as well as all molecules for which the energy error exceeds 0.3 kcal/mol (bottom). Data are taken from Table S2.

ered as entirely barrier-free. The third case concerns the imaginary frequency of the ring-opening mode for oxirene which is 93*i* cm^{-1} at the PBE0-D3/6-311G(d) level. Many methods share the problem of not identifying the C_{2v}-symmetric energy minimum,[103] reflecting the low barrier for rearrangement to formyl methylene,[141,142] and we find this to be true for 116 out of 219 methods studied here (see also Section 2.3). However, PBE0-D3/6-311G(d) still performs better than other density functionals, notably B3LYP with a range of basis sets,[104] which do not show any minimum for oxirene. PBE0-D3/6-311G(d) affords a second stationary point with C_s-symmetry (C−O: 1.425, 1.558 Å) that is a true minimum, about 0.02 kcal/mol lower in energy (and 0.15 kcal/mol higher at the B_5 level) than the C_{2v}-symmetric structure (C−O: 1.486 Å).

6.2. Error and Uncertainty Model for Geometries. Equation 1 defines the geometry error using exact energies and exact reference geometries. So far, we have adopted the final approximation of eq 2 instead, using a midlevel composite model (B_5) as energy probe and reference geometries that are near-optimal for that same level.

The evaluation of more accurate geometries is hardly feasible for the entire data set, but, as discussed in Section 3.1, probably not needed either: For 27 hydrocarbons, we used geometries fully optimized at the significantly more elaborate level of model A and saw little change in computed single-point B_5 energies, observing a difference of 0.1 kcal/mol in only one exceptional case. Looking for further confirmation, we have performed additional geometry optimizations at the B_5 and A levels, using the same procedure as in previous work,[38] now focusing on seven small molecules for which problems may be expected, including some for which PBE0-D3/6-311G(d) performs poorly. Table S5 lists geometry errors evaluated at the B_5 and A levels and based on reference geometries taken either from the pool ("best"), or from geometry optimizations at the B_5 and A levels. The effect of using fully optimized geometries rather than approximate ones reaches ≈0.1 kcal/mol in two cases: *cis*-FONO (compare Section 5) and F_2O_2, whose F−O bond length is known to be quite sensitive to basis set saturation and post-CCSD(T) effects.[143,144] Apart from these two extreme cases, the effect of fully optimizing the geometry is very small, and apart from only F_2O_2 the differences between using optimized B_5 and A geometries as reference to compute geometry errors of PBE0-D3/6-311G(d) are negligible. The latter observation again demonstrates the high quality of B_5 geometries and provides additional support for our choice to use this much simpler composite model as energy probe to select "best" geometries.

On the other hand, we anticipate some sensitivity of computed geometry errors to the level chosen for single-point energies, specifically in cases where the approximate geometry ($\tilde{G}_e^{k}[M]$) differs markedly from the reference geometry ($\tilde{G}_e^{k_{opt}}[M]$). Differences between models A and B_5 commonly reach 0.1 kcal/mol in those cases and even 0.2 kcal/mol for amineoxide (Table S5). To provide a refined data set to calibrate an empirical expression for $C_{A,e}^{geo}[M]$ and $u_{A,e}^{geo}[M]$ (eq 3), we have thus recomputed all geometry errors using "best" geometries ($\tilde{G}_e^{k_{opt}}[M]$) as reference and the more accurate model A as better approximation to the exact energy for single-point evaluations. The data listed in Table S2 (column "PBE0-D3") indicate a slight increase by 0.02 kcal/mol on average; larger shifts of up to about 0.2 kcal/mol are expectedly limited to a few molecules for which both composite models indicate significant geometry error (those discussed before as well as F_2NOF, see also Figure 5).

Using the refined data set (Table S2, column "PBE0-D3", subcolumn "A"), we see that geometry-related error remains below 0.1 kcal/mol in 62% and below 0.2 kcal/mol in 94% of all cases. The expected scaling with molecular size can be observed in a number of cases (e.g., 0.02 kcal/mol per carbon in *n*-alkanes, and per aromatic ring added to benzene), but the largest errors are observed for some smaller molecules containing bonds between heteroatoms (N, O, F); they exceed 0.3 kcal/mol in seven cases (Figure 5). Not all molecules with bonds between heteroatoms are problematic, but they do show larger error on average (0.17 kcal/mol for 63 molecules).

Unfortunately the presence of certain types of bonds is not always a good predictor of error. To give an example, the N−O bond in amineoxide is significantly too short at the PBE0-D3/6-311G(d) level (1.333 Å; reference: 1.360 Å, Table S5), giving rise to the largest error observed (0.67 kcal/mol, Figure 5), but the problem is much reduced in pyridine-*N*-oxide (1.257 Å, 1.270 Å, 0.18 kcal/mol) and nonexistent in trifluoramine oxide (1.153 Å, 1.154 Å, 0.02 kcal/mol, Table S5). Another example is the central N−O bond in the above-mentioned nitrosyl hypofluorite, much too short in the cis-isomer (1.362 Å, 1.426 Å, 0.48 kcal/mol, Table S5 and Figure 5), less so in the trans-isomer (1.470 Å, 1.492 Å, 0.22 kcal/

https://doi.org/10.1021/acs.jctc.1c00474
J. Chem. Theory Comput. 2021, 17, 4872−4890

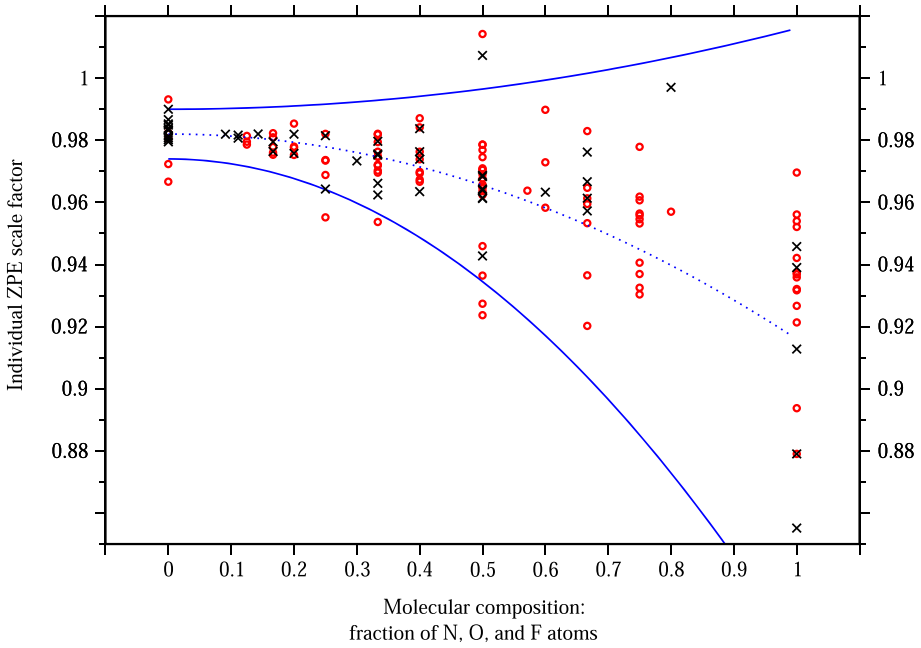

Figure 6. Individual ZPE scale factors for PBE0-D3/6-311G(d). Black crosses show the individual scale factor $f_{scal}^{(i)}$ needed to match a computed harmonic ZPE with anharmonic reference data. Red circles indicate the respective individual scale factor using scaled (0.9868, ref 131) harmonic CCSD(T)/cc-pVTZ data as reference instead. Data are plotted vs the fraction x_{NOF} of N, O, and F atoms contributing to the stoichiometry of a molecule. The blue dotted and solid lines indicate the final choice of corrected scale factors and related uncertainties adopted in the ATOMIC-2_{um} protocol (f_{scal}^{um}, eq 5). See Tables S3 and S6 for individual data.

mol). The problem is less severe in the related cis- (1.361 Å, 1.374 Å, 0.18 kcal/mol) and trans-isomers (1.400 Å, 1.416 Å, 0.09 kcal/mol) of nitrous acid (HONO).

Realizing that it is impossible to predict specific geometry errors with any confidence, we shall only try to estimate simple averages and ranges observed for molecules of given composition. Molecules not including heteroatoms, i.e., hydrocarbons and molecular hydrogen, are the easiest ones to deal with. Assigning small corrections of −0.005 and −0.01 kcal/mol to each hydrogen and carbon atom reduces the average error from 0.087 kcal/mol to a mere 0.006 kcal/mol, and the symmetric interval ranging from zero to twice the correction covers 96 out of 102 species (94%). Additional increments of −0.04 kcal/mol per N, O, and F atom are needed for the remaining 177 molecules that do include heteroatoms, reducing average error from 0.101 to 0.023 kcal/mol and covering 169 species (95%) in the interval ranging from zero to twice the correction.

Corrections and uncertainties are thus estimated from the number n_X of atoms of element X. Following a change of sign for application to atomization energies, they read

$$C_{A,e}^{geo}[M] = (n_H \cdot 0.005 + n_C \cdot 0.01 + (n_N + n_O + n_F) \cdot 0.04) \text{ kcal/mol}$$
$$u_{A,e}^{geo}[M] = \pm C_{A,e}^{geo}[M] \quad (4)$$

The model respects the expected and observed scaling with molecular size as well as the insight that any approximation to the true geometry must lower the atomization energy. The uncertainty interval covers 265 out of 279 molecules overall and so meets the goal of 95% confidence, while it reduces mean residual errors to negligible values (0.017 kcal/mol). As discussed above, the model is equally valid for two specific subsets (hydrocarbons, all other molecules, s.a.), but for obvious reasons, it may fail for sets focusing exclusively on molecules with many heteroatoms: For example, it covers just 36 of the 41 molecules (88%) containing only heteroatoms and hydrogen. Finally, we advise some caution in the interpretation of estimated error bars as observed errors cannot be expected to follow a symmetric normal distribution centered at $-C_{A,e}^{geo}[M]$. In fact, two-thirds rather than half of all observed errors (187 out of 279) are smaller and one-third are larger, an observation that we attribute to the quadratic scaling of energy with geometric displacement.

6.3. Error and Uncertainty Model for ZPEs. Some of the largest errors in scaled ZPEs ($ZPE^{scal} = f_{scal}ZPE$ = 0.979 ZPE) are observed for relatively small molecules (most notably ozone, 0.60 kcal/mol; Table S3, column "Error", "A"), while medium-sized organic molecules exhibit fairly small errors (e.g., molecules 30−34). Superficially, this observation would suggest that one estimates ZPE errors and uncertainties for out-of-set molecules from statistics obtained for the calibration set and neglects any possible size dependence. Such a proposal seems ill-advised, however, since many smaller frequency errors may add up to significant values for larger molecules. Note that the scarcity of good reference data does not really allow us to assess size dependence, benzene being the largest molecule in the set. Expressing uncertainties as a percentage of the ZPE would be desirable but faces the problem that some of the smaller molecules exhibit excessive relative errors (e.g., fluorine, difluoro monoxide, nitrous oxide, ozone: 4−14% of scaled ZPE, from data in Table S3), while others, such as hydrocarbons, do not (e.g., C_3H_n, all below 1% of scaled ZPE).

In developing the ATOMIC(hc) protocol, we were able to retain moderate percentage uncertainty intervals through the combination of two separate ZPE calculations, one at the MP2/cc-pVTZ level and another one at the B3LYP/cc-pVTZ level.[38] This choice was made based on the observation that

https://doi.org/10.1021/acs.jctc.1c00474
J. Chem. Theory Comput. 2021, 17, 4872−4890

both levels afford acceptable results overall, but often err on opposite sides. Not only does the averaging of scaled ZPEs improve final statistics, but differences between individual results serve as a sanity check allowing us to identify problem cases and increase moderate default uncertainties of 0.8% uncertainties accordingly such that the overall goal of 95% confidence intervals is (nearly) met. This approach appears to work well in general; however, the addition of a second geometry optimization and force constant calculation compromises simplicity and efficiency of the thermochemistry protocol. It has thus not been considered as an option for ATOMIC-2.

Figure 6 analyzes individual scale factors $f_{scal}^{(i)}$ determined to match the target ZPE of molecule i precisely. Black crosses show $f_{scal}^{(i)}$ values as a function of molecular composition, using x_{NOF} as dependent variable, which expresses the fraction of heteroatoms, i.e., the total number of N, O, and F atoms divided by the total number of all atoms. Individual scale factors for molecules with low heteroatom content fall into a narrow range around 0.98, those for molecules with larger heteroatom content vary widely and are significantly smaller on average. This observation suggests that errors in computed vibrational frequencies may be relatively consistent for certain types of vibrational modes (involving C and H atoms) but not necessarily in general. It may also reflect the larger size of organic molecules (small x_{NOF}) in the calibration set, which infers a larger number of different modes and so enhanced chances of error cancellation between over- and underestimated contributions to the ZPE.[38]

Least-squares fits for molecules with $x_{NOF} = 0$ or 1 yield $f_{scal,0} = 0.982$ (11 data) and $f_{scal,1} = 0.916$ (5 data), respectively, and we find that a quadratic function, $f_{scal}^{um} = 0.982 - 0.066 \cdot x_{NOF}^2$ interpolates reasonably well between the extreme points $x_{NOF} = 0$ and 1. We estimate the uncertainty as ±0.8% of the unscaled ZPE for $x_{NOF} = 0$, which (just) covers all data for molecules without heteroatoms and as ±10% for $x_{NOF} = 1$ such that the combined estimate

$$f_{scal}^{um} = (0.982 - 0.066 \cdot x_{NOF}^2) \pm (0.008 + 0.092 \cdot x_{NOF}^2) \quad (5)$$

covers all molecules but one (hydrogen fluoride) and so meets our goal of 95% or better uncertainty intervals. Equation 5 is the final definition of the scale factor f_{scal}^{um} adopted in the ATOMIC-2_{um} uncertainty model, and so the terms

$$C^{ZPE}[M] = (0.003 - 0.066 \cdot x_{NOF}^2)\text{ZPE}$$
$$u^{ZPE}[M] = \pm(0.008 + 0.092 \cdot x_{NOF}^2)\text{ZPE} \quad (6)$$

estimate bias and uncertainty of the scaled harmonic value, f_{scal}ZPE = 0.979·ZPE used in regular ATOMIC-2. The proposed bias correction is quite effective; it reduces mean signed and RMS errors from 0.06 and 0.21 kcal/mol for the set (Table S4) to −0.01 kcal/mol and 0.15 kcal/mol, respectively.

6.4. Validation of Error and Uncertainty Model for ZPEs. We have obtained harmonic ZPEs at the CCSD(T)/cc-pVTZ level for all 99 molecules considered earlier at the same level for geometry optimizations (Section 3.1). Scaled ZPEs are expectedly more reliable at this level (f_{scal} = 0.9868[131]) than at density functional levels (Table S3), prompting us to use them as auxiliary reference. Individual scale factors $f_{scal}^{(i)}$ determined with this reference for PBE0-D3/6-311G(d) are shown as red circles in Figure 6. They confirm trends already observed with accurate anharmonic reference data (black crosses), but now for a larger set of molecules: With increasing heteroatom content, $f_{scal}^{(i)}$ tends to smaller values on average and shows a larger variance between molecules. There are eight molecules with $f_{scal}^{(i)}$ values outside the uncertainty estimate (blue solid lines in Figure 6): two molecules above the upper limit (hydrogen fluoride, s.a., and hydrogen) and six molecules below, all with CC and CN triple bonds, for which reference values appear to underestimate true anharmonic ZPEs, however, as explained below.

Table S6 further compares ATOMIC-2_{um} ZPEs to the set of scaled CCSD(T)/cc-pVTZ ZPEs just discussed, and to three different estimates for the entire 279 molecule test set,[145] each believed to be more accurate than PBE0-D3/6-311G(d): the model implemented in ATOMIC(hc),[38] the method performing best for the calibration set (TPSSh/TZVP, RMS error: 0.130 kcal/mol), and the pair of methods whose average shows the best performance for the calibration set (MN12-L/6-31G(d) and TPSS/TZVP, RMS = 0.105 kcal/mol), not far from the accuracy of typical double-hybrid functionals (RMS ≈ 0.09 kcal/mol, bottom of Table S4). Figure 7 illustrates

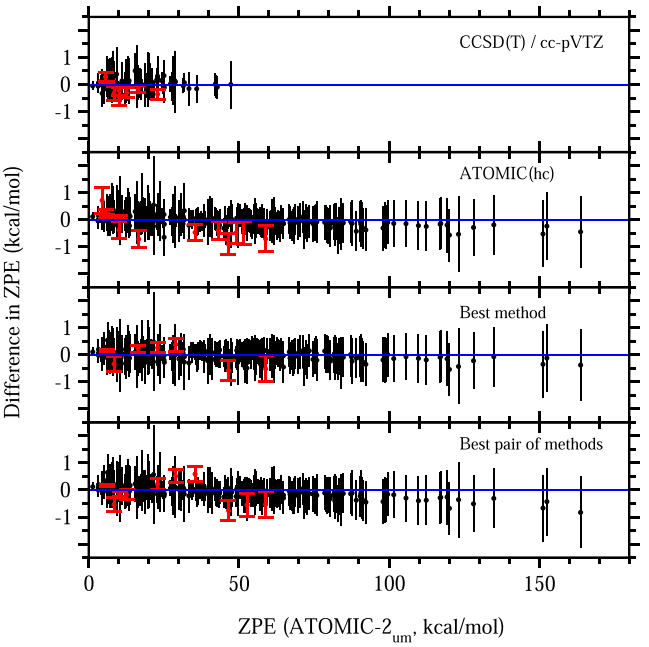

Figure 7. Difference between scaled harmonic ZPEs from a variety of sources and those defined for ATOMIC-2_{um}. The sources are (a) CCSD(T)/cc-pVTZ, (b) ATOMIC(hc) (ref 38), (c) method showing the smallest RMS error for the calibration set after scaling (TPSSh/TZVP; 0.130 kcal/mol), and (d) the pair of methods with the smallest RMS error after scaling and averaging (MN12-L/6-31G(d), TPSS/TZVP; 0.105 kcal/mol). ATOMIC-2_{um} data are shown with error bars. Cases for which differences exceed error bars are highlighted in red. See Table S6 for individual data.

comparisons in graphical form and highlights cases of disagreement in red color (also marked in Table S6). There are 19 potential problem cases (6.8% of 279), for which ATOMIC-2_{um} error bars do not enclose all available external reference data: These include the known outlier hydrogen fluoride (s.a.), but also four molecules (hydrogen cyanide, singlet methylene, acetylene, ozone), for which accurate anharmonic ZPEs are covered by ATOMIC-2_{um} error bars as Table S3 shows.

https://doi.org/10.1021/acs.jctc.1c00474
J. Chem. Theory Comput. 2021, 17, 4872−4890

Many of the problem cases involve molecules with CC and CN triple bonds. For six of them, we have scaled CCSD(T)/cc-pVTZ data available (# 14, 49, 53, 56, 85, 104), all of which are below the lower end of ATOMIC-2_{um} uncertainty intervals but almost certainly also below true anharmonic ZPEs. We have verified this for hydrogen cyanide (#14) and acetylene (#56, above) and expect this to be true also for the remaining four species. Based on published high-quality experimental and theoretical data for harmonic and fundamental frequencies, we may estimate anharmonic ZPEs as weighted averages (5/8 ZPE^{harm} + 3/8 ZPE^{fund}).[146] In particular, we find ZPE^{harm} = 8.20,[147] 12.54,[148] 9.88,[149] and 23.06 kcal/mol[150] for difluoroacetylene (#49), fluoroacetylene (#53), cyanogen (#85), and 1,3-butadiyne (#104), respectively, and ZPE^{fund} = 8.08,[151] 12.23,[152] 9.73,[153] and 22.39 kcal/mol.[150] In all of these cases, derived estimates of anharmonic ZPEs (8.16, 12.42, 9.82, 22.81 kcal/mol) are slightly larger than scaled CCSD(T)/cc-pVTZ values (8.11, 12.35, 9.69, 22.57 kcal/mol, Table S6) and so either within or at least closer to the boundaries of ATOMIC-2_{um} uncertainty intervals (8.44 ± 0.27, 12.64 ± 0.18, 10.13 ± 0.33, 22.93 ± 0.19 kcal/mol, Table S6).

In summary, the assessment does not raise any concerns about the choice of ATOMIC-2_{um} uncertainty estimates. Of course, it is only a consistency check and does not replace rigorous benchmark evaluations, which would have been preferable but cannot be accomplished in the absence of a large base of accurate reference data. The assessment still suggests that the proposed error and uncertainty model achieves the set goal of providing 95% (or better) confidence intervals, which is encouraging since estimated error bars are fairly moderate overall and exceed 1 kcal/mol in only 17 out of 279 cases, including some larger hydrocarbons.

Irikura et al. have reported standard uncertainties (1σ) of 0.02 and more for ZPE scale factors of a range of wave function and density functional methods.[154] Although the validity of such statistical analysis has been discussed controversially,[155,156] the final message is clear: scaled ZPEs may carry errors of several percent, which would make them almost useless for many thermochemistry applications. Here, we have developed an entirely empirical uncertainty model that analyzes observations in terms of individual scale factors $f_{scal}^{(i)}$. It suggests that the problem is far less severe for typical organic molecules, a major focus for applications of ATOMIC-2, but that large percentage uncertainties need to be accepted for molecules with high heteroatom content. Luckily the latter often carry small ZPEs, so estimated uncertainties remain moderate in absolute terms. The most extreme case among the 279 molecules studied here is carbonyl diazide; it shows the largest estimated error bar overall (±1.82 kcal/mol, # 46, Table S6).

The observed difference in percentage accuracy between molecules with low and high heteroatom contents is not limited to the chosen model PBE0-D3/6-311G(d), but it is in fact quite common among all approaches analyzed here. To demonstrate this, we split the benchmark set of 50 molecules into two subsets for analysis, one (A) with 27 molecules of low heteroatom content ($x_{NOF} < 0.4$), the other (B) with 23 molecules of high heteroatom content ($x_{NOF} \geq 0.4$). Table S4 shows that individual scale factors, averaged over the first set ($\overline{f_{scal}^{(i)}}$, A) nearly always reproduce optimized scale factors (f_{scal}) to within ±0.002 and carry small standard deviations below 0.01, while those averaged over the second subset ($\overline{f_{scal}^{(i)}}$, B) often deviate substantially and typically carry standard deviations larger than 0.03.

7. DISCUSSION AND CONCLUSIONS

We have assessed 53 density functionals, HF and MP2 for their utility to optimize geometries and evaluate zero-point energies (ZPEs) in thermochemistry protocols. The goal has been to compare computationally efficient approaches, assess currently popular options, and identify interesting candidates that provide good accuracy and reliability at a low cost. Hence, we have focused on density functionals of the first four rungs as well as on fairly small basis sets, discarding the idea to assess intrinsic accuracies of functionals at their basis set limits.

Optimized geometries are probed with single-point energy evaluations at the ATOMIC/B_5 level, which is known to be reliable for relative energies (such as bond separation energies) and serve as a good approximation to the complete basis set limit of CCSD(T) with all electrons correlated. The assembly of a large data set even obviates the need for expensive geometry optimizations at this level to generate reference data: Each of the 219 probed methods contributes one geometry and so one particular point to the B_5 potential energy surface of a molecule (Figure 1), and the geometry of lowest energy is known to be the best available approximation of a fully optimized geometry. Limited comparison to external references demonstrates that this procedure indeed generates quite accurate geometries, superior even to fully optimized CCSD(T)(fc)/cc-pVTZ geometries (Section 3.1). The use of a midlevel composite model (B_5) as reference and the lack of full optimization at the reference level may preclude very precise estimates of geometry-related energy error for seriously displaced geometries (Section 6.2). The largely harmonic nature of potential energy surfaces ensures, however, that the assessment is accurate where it needs to be to identify good candidates for geometry optimization: in the estimate of energy error for geometries close to the true energy minimum (Section 6.2).

The benchmark contains 279 molecules composed of first-row atoms (H, C, N, O, F) and deliberately includes some larger species as well as difficult cases such as molecules with high angular strain or known multireference character. Among a total of 61 100 optimized geometries, we find 3444 cases with energy penalties larger than 1 kcal/mol, involving 133 (of 219) methods and 252 (of 279) molecules. Energy penalties even exceed 2 kcal/mol in 879 cases, involving 81 methods and 115 molecules. Errors of this magnitude are obviously unacceptable for thermochemical applications. No functional of the first two rungs satisfies even modest expectations, and one needs to resort to the best-performing hybrid functionals for excellent results (Figure 2). Small polarized basis sets (6-31G(d)) are sufficient, slightly larger basis sets (6-311G(d)) are often better, but further basis set extension is not always warranted (Section 3.2 and Figure 4).

ZPE scale factors have been obtained for a subset of 50 molecules, for which accurate (anharmonic) reference data are available. Assessment for the same set shows that well-performing functionals can be found among all four rungs and that basis set requirements are modest (6-31G(d), Figure 3). Some functionals do perform poorly, but not nearly to the extent that we have observed for geometries. On the other hand, also best performance (RMS error: 0.13 kcal/mol, Table

https://doi.org/10.1021/acs.jctc.1c00474
J. Chem. Theory Comput. 2021, 17, 4872−4890

S4) lags behind that achievable for geometries (0.09 kcal/mol, Table S1), and this is for a benchmark containing substantially smaller molecules on average (5.2 vs 9.5 atoms per molecule). Further analysis shows that all density functionals, but also HF and MP2, exhibit larger percentage ZPE errors for molecules with a high heteroatom content (Section 6.4). Since the relevant subset contains even smaller molecules on average (3.6 atoms per molecule, $x_{NOF} \geq 0.4$) with just a few vibrational modes and correspondingly small ZPEs, it is not adequately represented in reported overall RMS errors, which therefore may be poor predictors of performance for practical applications to larger molecules with high heteroatom content. This discussion allows two conclusions: First, ZPE error will generally dominate over geometry-related error for as long as we select a method known to be good at geometries. Second, the RMS statistics for ZPEs need to be interpreted with some caution, and uncertainty estimates for molecules with high heteroatom content need to be liberal, reflecting observations as well as unavoidable limitations of our assessment.

Balancing performance for geometries and ZPEs, there are a number of density functionals that promise to be good candidates for wave function-based thermochemistry protocols (Figure 4). Most of them are hybrid functionals as moderate amounts of exact exchange often improve accuracies of optimized geometries. It is striking to see that some of the oldest hybrid functionals with no or just a few empirically fit parameters are among the best options (e.g., B1B95, B3P86, B3LYP, B3PW91, mPW1PW91, mPW1PBE, mPW3PBE, PBE0), while a number of highly parametrized functionals (Minnesota functionals, BMK) perform notably worse. B3LYP has not only been—and still is—one of the most popular representatives in chemistry, it is also one of the top performers for geometries and ZPEs, provided that basis sets with multiple polarization functions are used such as in Gaussian-4 (6-31G(2df,p)) and in lower-level variants of the Weizmann protocol (cc-pVTZ). Some other functionals provide excellent performance already for smaller basis sets, which is of course preferable for overall computational efficiency.

We have selected PBE0-D3/6-311G(d) for the next version of the ATOMIC protocol. It uses a small basis set, shows excellent performance for geometries, is largely nonempirical, and is widely available in computational chemistry software. The dispersion correction (D3) has a negligible effect for small- to medium-sized molecules and may be omitted if desired, but promises better accuracy for larger systems as demonstrated for an ensemble of 10 alanine tetrapeptide conformations. The chosen protocol shows only average performance for ZPEs (Table S4), but it never fails badly: The difference between maximum positive and negative errors amounts to 0.87 kcal/mol, not much worse than the best option (N12/6-31G(d), 0.69 kcal/mol) but superior to MP2/cc-pVTZ (1.95 kcal/mol), which it is set to replace in the update of the ATOMIC protocol.

Compared to MP2/cc-pVTZ it shows even more performance gain in geometries (RMS and MAX: 0.11 and 0.58 kcal/mol *vs* 0.30 and 2.04 kcal/mol, Tables S1 and S2), which is also visible in statistics for all 2526 bond lengths (error range: −0.065 to 0.033 Å, RMS: 0.005 Å *vs* −0.133 to 0.070 Å, 0.007 Å). Apart from this, it is much more efficient computationally than MP2/cc-pVTZ, easily saving an order of magnitude in running time for geometry optimizations and ZPE evaluations of mid-sized molecules, turning the computational bottleneck of the ATOMIC protocol into a low-effort component. Using single-threaded codes (Section 2.3) on commodity hardware, our benchmark took a total of 2.2 days to run a complete set of 279 single-point B_5 evaluations, 1 day for all preceding geometry optimizations and frequency calculations in the case of PBE0-D3/6-311G(d), but nearly 2 months in the case of MP2/cc-pVTZ.

Most remaining problems are observed for geometries and ZPEs of molecules with several heteroatoms (Sections 6.2 and 6.4). We propose simple size-extensive error and uncertainty models that accommodate this insight (eqs 4 and 6) and estimate average bias as well as error bars that correspond to intervals of 95% confidence. Bias correction reduces the RMS error observed for ZPEs from 0.21 to 0.15 kcal/mol and so depletes the disadvantage of PBE0-D3/6-311G(d) relative to the best-performing functionals (RMS ≈ 0.13 kcal/mol). We note that the same approach improves error statistics for a number of other functionals, too, but that it does not affect achievable top-performance (best: MN12-L/6-31G(d): 0.127 kcal/mol; details not shown).

The lack of a large and reliable reference data set precludes rigorous validation of the uncertainty model for ZPEs, but comparison with alternative approximate ZPE evaluations, each believed to be more accurate than PBE0-D3/6-311G(d), indicates that it provides a fair estimate of 95% confidence (Section 6.4). Applied to the 279 molecule benchmark (Table S6), estimated uncertainties average to 0.57 kcal/mol, which is certainly acceptable for thermochemical protocols targeting chemical accuracy overall (≈1 kcal/mol). Uncertainties relating to geometry error are expectedly much smaller on average (0.11 kcal/mol, Table S2) and almost negligible in thermochemical applications.

■ ASSOCIATED CONTENT

Supporting Information

The Supporting Information is available free of charge at https://pubs.acs.org/doi/10.1021/acs.jctc.1c00474.

Method performance for geometry optimization, geometry errors for selected methods and all molecules, reference and selected other data for zero-point energies (ZPEs), method performance for ZPEs, highly accurate geometries for selected molecules (Tables S1−S5), and comparison of ZPEs evaluated with selected methods for the complete set of molecules (Table S6) (PDF)

All optimized geometries relating to Tables S1 and S2, corresponding vibrational frequencies, and B_5 composite energies (ZIP)

■ AUTHOR INFORMATION

Corresponding Author

Dirk Bakowies − *Institute of Physical Chemistry, Department of Chemistry, University of Basel, CH 4056 Basel, Switzerland;* orcid.org/0000-0002-8787-6990; Email: dbakowies@gmail.com

Author

O. Anatole von Lilienfeld − *Faculty of Physics, University of Vienna, A 1090 Vienna, Austria; Institute of Physical Chemistry and National Center for Computational Design and Discovery of Novel Materials (MARVEL), Department of Chemistry, University of Basel, CH 4056 Basel, Switzerland*

Complete contact information is available at:
https://pubs.acs.org/10.1021/acs.jctc.1c00474

Notes

The authors declare no competing financial interest.

■ ACKNOWLEDGMENTS

This work was generously supported by a grant from the Swiss National Supercomputing Centre (CSCS) under project ID s152. Some calculations were performed at the sciCORE (http://scicore.unibas.ch/) scientific computing center of University of Basel. Support from the European Research Council is acknowledged (ERC-CoG grant QML #772834, and H2020 projects BIG-MAP and TREX under Grant Agreements #952165 and #957189). This result only reflects the author's view, and the EU is not responsible for any use that may be made of the information it contains. The authors also acknowledge support by the NCCR MARVEL, funded by the Swiss National Science Foundation.

■ REFERENCES

(1) Pople, J. A.; Head-Gordon, M.; Fox, D. J.; Raghavachari, K.; Curtiss, L. A. Gaussian-1 theory: A general procedure for prediction of molecular energies. *J. Chem. Phys.* **1989**, *90*, 5622−5629.
(2) Curtiss, L. A.; Raghavachari, K.; Trucks, G. W.; Pople, J. A. Gaussian-2 theory for molecular energies of first- and second-row compounds. *J. Chem. Phys.* **1991**, *94*, 7221−7230.
(3) Curtiss, L. A.; Raghavachari, K.; Redfern, P. C.; Rassolov, V.; Pople, J. A. Gaussian-3 (G3) theory for molecules containing first and second-row atoms. *J. Chem. Phys.* **1998**, *109*, 7764−7776.
(4) Curtiss, L. A.; Redfern, P. C.; Raghavachari, K. Gaussian-4 theory. *J. Chem. Phys.* **2007**, *126*, No. 084108.
(5) Ochterski, J. W.; Petersson, G. A.; Montgomery, J. A., Jr. A complete basis set model chemistry. V. Extensions to six or more heavy atoms. *J. Chem. Phys.* **1996**, *104*, 2598−2619.
(6) Karton, A.; Ruscic, B.; Martin, J. M. L. Benchmark atomization energy of ethane: Importance of accurate zero-point vibrational energies and diagonal Born-Oppenheimer corrections for a 'simple' organic molecule. *J. Mol. Struct.: THEOCHEM* **2007**, *811*, 345−353.
(7) Chan, B. How to computationally calculate thermochemical properties objectively, accurately, and as economically as possible. *Pure Appl. Chem.* **2017**, *89*, 699−713.
(8) Møller, C.; Plesset, M. S. Note on an approximation treatment for many-electron systems. *Phys. Rev.* **1934**, *46*, 618−622.
(9) Becke, A. D. A new mixing of Hartree-Fock and local density-functional theories. *J. Chem. Phys.* **1993**, *98*, 1372−1377.
(10) Becke, A. D. Density-functional thermochemistry. III. The role of exact exchange. *J. Chem. Phys.* **1993**, *98*, 5648−5652.
(11) Bauschlicher, C. W.; Partridge, H. A modification of the Gaussian-2 approach using density functional theory. *J. Chem. Phys.* **1996**, *105*, 1788−1791.
(12) Curtiss, L. A.; Raghavachari, K.; Redfern, P. C.; Pople, J. A. Investigation of the use of B3LYP zero-point energies and geometries in the calculation of enthalpies of formation. *Chem. Phys. Lett.* **1997**, *270*, 419−426.
(13) Baboul, A. G.; Curtiss, L. A.; Redfern, P. C.; Raghavachari, K. Gaussian-3 theory using density functional geometries and zero-point energies. *J. Chem. Phys.* **1999**, *110*, 7650−7657.
(14) Stephens, P. J.; Devlin, F. J.; Chabalowski, C. F.; Frisch, M. J. Ab initio calculation of vibrational absorption and circular dichroism spectra using density functional force fields. *J. Phys. Chem.* **1994**, *98*, 11623−11627.
(15) Montgomery, J. A.; Frisch, M. J.; Ochterski, J. W.; Petersson, G. A. A complete basis set model chemistry. VI. Use of density functional geometries and frequencies. *J. Chem. Phys.* **1999**, *110*, 2822−2827.
(16) Krishnan, R.; Binkley, J. S.; Seeger, R.; Pople, J. A. Self-consistent molecular orbital methods. 20. A basis set for correlated wave functions. *J. Chem. Phys.* **1980**, *72*, 650−654.
(17) Frisch, M. J.; Pople, J. A.; Binkley, J. S. Self-consistent molecular orbital methods. 25. Supplementary functions for Gaussian basis sets. *J. Chem. Phys.* **1984**, *80*, 3265−3269.
(18) DeYonker, N. J.; Cundari, T. R.; Wilson, A. K. The correlation consistent composite approach (ccCA): An alternative to the Gaussian-n methods. *J. Chem. Phys.* **2006**, *124*, No. 114104.
(19) Hariharan, P. C.; Pople, J. A. The effect of d-functions on molecular orbital energies for hydrocarbons. *Chem. Phys. Lett.* **1972**, *16*, 217−219.
(20) Martin, J. M. L.; de Oliveira, G. Towards standard methods for benchmark quality ab initio thermochemistry - W1 and W2 theory. *J. Chem. Phys.* **1999**, *111*, 1843−1856.
(21) Karton, A.; Kaminker, I.; Martin, J. M. L. Economical post-CCSD(T) computational thermochemistry protocol and applications to some aromatic compounds. *J. Phys. Chem. A* **2009**, *113*, 7610−7620.
(22) Dunning, T. H., Jr. Gaussian basis sets for use in correlated molecular calculations. I. The atoms boron through neon and hydrogen. *J. Chem. Phys.* **1989**, *90*, 1007−1023.
(23) Boese, A. D.; Martin, J. M. L. Development of density functionals for thermochemical kinetics. *J. Chem. Phys.* **2004**, *121*, 3405−3416.
(24) Chan, B.; Deng, J.; Radom, L. G4(MP2)-6X: A cost-effective improvement to G4(MP2). *J. Chem. Theory Comput.* **2011**, *7*, 112−120.
(25) Chan, B.; Karton, A.; Raghavachari, K. G4(MP2)-XK: A variant of the G4(MP2)-6X composite method with expanded applicability for main-group elements up to radon. *J. Chem. Theory Comput.* **2019**, *15*, 4478−4484.
(26) Sousa, S. F.; Fernandes, P. A.; Ramos, M. J. General performance of density functionals. *J. Phys. Chem. A* **2007**, *111*, 10439−10452.
(27) Peverati, R.; Truhlar, D. G. Quest for a universal density functional: The accuracy of density functionals across a broad spectrum of databases in chemistry and physics. *Philos. Trans. R. Soc., A* **2014**, *372*, No. 20120476.
(28) Mardirossian, N.; Head-Gordon, M. Thirty years of density functional theory in computational chemistry: an overview and extensive assessment of 200 density functionals. *Mol. Phys.* **2017**, *115*, 2315−2372.
(29) Riley, K. E.; Op't Holt, B. T.; Merz, K. M. Critical assessment of the performance of density functional methods for several atomic and molecular properties. *J. Chem. Theory Comput.* **2007**, *3*, 407−433.
(30) Brémond, E.; Savarese, M.; Su, N. Q.; Pérez-Jiménez, Á. J.; Xu, X.; Sancho-García, J. C.; Adamo, C. Benchmarking density functionals on structural parameters of small-/medium-sized organic molecules. *J. Chem. Theory Comput.* **2016**, *12*, 459−465.
(31) Chan, B. Use of low-cost quantum chemistry procedures for geometry optimization and vibrational frequency calculations: Determination of frequency scale factors and application to reactions of large systems. *J. Chem. Theory Comput.* **2017**, *13*, 6052−6060.
(32) Vuckovic, S.; Burke, K. Quantifying and understanding errors in molecular geometries. *J. Phys. Chem. Lett.* **2020**, *11*, 9957−9964.
(33) Model B_S augments the valence-shell MP2 energy, evaluated from cc-pVTZ and cc-pVQZ basis sets and extrapolated to the complete-basis-set limit, with MP2 core-valence corrections at the triple-ζ level and small basis set evaluations of valence-shell CCSD-MP2 and CCSD(T)-CCSD increments. Either one of the latter employs unpolarized cc-pVDZ on hydrogen, combined with the (spd) set of cc-pVTZ (CCSD-MP2) or regular cc-pVDZ (CCSD(T)-CCSD) on first-row atoms. The more advanced model A employs complete-basis set extrapolations for all valence-shell components (MP2: (Q5), CCSD-MP2: (TQ), CCSD(T)-CCSD: (DT)). See refs 34 and 36 for details.

(34) Bakowies, D. Ab initio thermochemistry using optimal-balance models with isodesmic corrections: The ATOMIC protocol. *J. Chem. Phys.* **2009**, *130*, No. 144113.
(35) Bakowies, D. Ab initio thermochemistry with high-level isodesmic corrections: Validation of the ATOMIC protocol for a large set of compounds with first-row atoms (H, C, N, O, F). *J. Phys. Chem. A* **2009**, *113*, 11517−11534.
(36) Bakowies, D. Simplified wave function models in thermochemical protocols based on bond separation reactions. *J. Phys. Chem. A* **2014**, *118*, 11811−11827.
(37) Bakowies, D. Estimating systematic error and uncertainty in ab initio thermochemistry: I. Atomization energies of hydrocarbons in the ATOMIC(hc) protocol. *J. Chem. Theory Comput.* **2019**, *15*, 5230−5251.
(38) Bakowies, D. Estimating systematic error and uncertainty in ab initio thermochemistry: II. ATOMIC(hc) enthalpies of formation for a large set of hydrocarbons. *J. Chem. Theory Comput.* **2020**, *16*, 399−426.
(39) Ditchfield, R.; Hehre, W. J.; Pople, J. A.; Radom, L. Molecular orbital theory of bond separation. *Chem. Phys. Lett.* **1970**, *5*, 13−14.
(40) Hehre, W. J.; Ditchfield, R.; Radom, L.; Pople, J. A. Molecular orbital theory of the electronic structure of organic compounds. V. Molecular theory of bond separation. *J. Am. Chem. Soc.* **1970**, *92*, 4796−4801.
(41) Weigend, F.; Häser, M. RI-MP2: First derivatives and global consistency. *Theor. Chem. Acc.* **1997**, *97*, 331−340.
(42) Adamo, C.; Barone, V. Toward reliable density functional methods without adjustable parameters: The PBE0 model. *J. Chem. Phys.* **1999**, *110*, 6158−6170.
(43) Ernzerhof, M.; Scuseria, G. E. Assessment of the Perdew-Burke-Ernzerhof exchange-correlation functional. *J. Chem. Phys.* **1999**, *110*, 5029−5036.
(44) Perdew, J. P.; Ernzerhof, M.; Burke, K. Rationale for mixing exact exchange with density functional approximations. *J. Chem. Phys.* **1996**, *105*, 9982−9985.
(45) Grimme, S.; Antony, J.; Ehrlich, S.; Krieg, H. A consistent and accurate ab initio parametrization of density functional dispersion correction (DFT-D) for the 94 elements H-Pu. *J. Chem. Phys.* **2010**, *132*, No. 154104.
(46) Perdew, J. P.; Schmidt, K. Jacob's ladder of density functional approximations for the exchangecorrelation energy, In *Density Functional Theory and Its Application to Materials*, Vol. 577 of AIP Conference Proceedings, van Doren, V.; van Alsenoy, C.; Geerlings, P., Eds.; 2001; pp 1−20.
(47) Slater, J. C. *The Self-Consistent Field for Molecules and Solids: Quantum Theory of Molecules and Solids*; Mc Graw Hill: New York, 1974; Vol. *4*.
(48) Vosko, S. H.; Wilk, L.; Nusair, M. Accurate spin-dependent electron liquid correlation energies for local spin density calculations: A critical analysis. *Can. J. Phys.* **1980**, *58*, 1200−1211.
(49) Becke, A. D. Density-functional exchange-energy approximation with correct asymptotic behavior. *Phys. Rev. A* **1988**, *38*, 3098−3100.
(50) Lee, C.; Yang, W.; Parr, R. G. Development of the Colle-Salvetti correlation-energy formula into a functional of the electron density. *Phys. Rev. B* **1988**, *37*, 785−789.
(51) Perdew, J. P. Density-functional approximation for the correlation energy of the inhomogeneous electron gas. *Phys. Rev. B* **1986**, *33*, 8822−8824.
(52) Hamprecht, F. A.; Cohen, A. J.; Tozer, D. J.; Handy, N. C. Development and assessment of new exchange-correlation functionals. *J. Chem. Phys.* **1998**, *109*, 6264−6271.
(53) Boese, A. D.; Handy, N. C. A new parametrization of exchange-correlation generalized gradient approximation functionals. *J. Chem. Phys.* **2001**, *114*, 5497−5503.
(54) Perdew, J. P.; Burke, K.; Ernzerhof, M. Generalized gradient approximation made simple. *Phys. Rev. Lett.* **1996**, *77*, 3865−3868.
(55) Peverati, R.; Zhao, Y.; Truhlar, D. G. Generalized gradient approximation that recovers the second-order density-gradient expansion with optimized across-the-board performance. *J. Phys. Chem. Lett.* **2011**, *2*, 1991−1997.
(56) Grimme, S. Semiempirical GGA-type density functional constructed with a long-range dispersion correction. *J. Comput. Chem.* **2006**, *27*, 1787−1799.
(57) Grimme, S.; Ehrlich, S.; Goerigk, L. Effect of the damping function in dispersion corrected density functional theory. *J. Comput. Chem.* **2011**, *32*, 1456−1465.
(58) Zhao, Y.; Truhlar, D. G. A new local density functional for main-group thermochemistry, transition metal bonding, thermochemical kinetics, and noncovalent interactions. *J. Chem. Phys.* **2006**, *125*, No. 194101.
(59) Peverati, R.; Truhlar, D. G. M11-L: A local density functional that provides improved accuracy for electronic structure calculations in chemistry and physics. *J. Phys. Chem. Lett.* **2012**, *3*, 117−124.
(60) Peverati, R.; Truhlar, D. G. An improved and broadly accurate local approximation to the exchange-correlation density functional: The MN12-L functional for electronic structure calculations in chemistry and physics. *Phys. Chem. Chem. Phys.* **2012**, *14*, 13171−13174.
(61) Peverati, R.; Truhlar, D. G. Exchange-correlation functional with good accuracy for both structural and energetic properties while depending only on the density and its gradient. *J. Chem. Theory Comput.* **2012**, *8*, 2310−2319.
(62) Tao, J.; Perdew, J. P.; Staroverov, V. N.; Scuseria, G. E. Climbing the density functional ladder: Nonempirical meta-generalized gradient approximation designed for molecules and solids. *Phys. Rev. Lett.* **2003**, *91*, No. 146401.
(63) van Voorhis, T.; Scuseria, G. E. A novel form for the exchange-correlation energy functional. *J. Chem. Phys.* **1998**, *109*, 400−410.
(64) Austin, A.; Petersson, G. A.; Frisch, M. J.; Dobek, F. J.; Scalmani, G.; Throssell, K. A density functional with spherical atom dispersion terms. *J. Chem. Theory Comput.* **2012**, *8*, 4989−5007.
(65) Becke, A. D. Density-functional thermochemistry. IV. A new dynamical correlation functional and implications for exact-exchange mixing. *J. Chem. Phys.* **1996**, *104*, 1040−1046.
(66) Adamo, C.; Barone, V. Toward reliable adiabatic connection models free from adjustable parameters. *Chem. Phys. Lett.* **1997**, *274*, 242−250.
(67) Wilson, P. J.; Bradley, T. J.; Tozer, D. J. Hybrid exchange-correlation functional determined from thermochemical data and ab initio potentials. *J. Chem. Phys.* **2001**, *115*, 9233−9242.
(68) Chai, J.-D.; Head-Gordon, M. Systematic optimization of long-range corrected hybrid density functionals. *J. Chem. Phys.* **2008**, *128*, No. 084106.
(69) Chai, J.-D.; Head-Gordon, M. Long-range corrected hybrid density functionals with damped atom-atom dispersion corrections. *Phys. Chem. Chem. Phys.* **2008**, *10*, 6615−6620.
(70) Schmider, H. L.; Becke, A. D. Optimized density functionals from the extended G2 test set. *J. Chem. Phys.* **1998**, *108*, 9624−9631.
(71) Frisch, M. J.; Trucks, G. W.; Schlegel, H. B.; Scuseria, G. E.; Robb, M. A.; Cheeseman, J. R.; Scalmani, G.; Barone, V.; Mennucci, B.; Petersson, G. A. et al. *Gaussian 09*, revision D.01; Gaussian, Inc.: Wallingford, CT.
(72) BHandH and BHandHLYP are unpublished "half and half" hybrid functionals defined only in the user manual to the Gaussian system of programs (ref 71).
(73) Yanai, T.; Tew, D. P.; Handy, N. C. A new hybrid exchange-correlation functional using the Coulomb-attenuating method (CAM-B3LYP). *Chem. Phys. Lett.* **2004**, *393*, 51−57.
(74) Boese, A. D.; Handy, N. C. New exchange-correlation density functionals: The role of the kinetic-energy density. *J. Chem. Phys.* **2002**, *116*, 9559−9569.
(75) Henderson, T. M.; Izmaylov, A. F.; Scuseria, G. E.; Savin, A. The importance of middle-range Hartree-Fock-type exchange for hybrid density functionals. *J. Chem. Phys.* **2007**, *127*, No. 221103.
(76) Henderson, T. M.; Izmaylov, A. F.; Scuseria, G. E.; Savin, A. Assessment of a middle-range hybrid functional. *J. Chem. Theory Comput.* **2008**, *4*, 1254−1262.

https://doi.org/10.1021/acs.jctc.1c00474
J. Chem. Theory Comput. 2021, 17, 4872−4890

(77) Heyd, J.; Scuseria, G. E.; Ernzerhof, M. Hybrid functionals based on a screened Coulomb potential. *J. Chem. Phys.* **2003**, *118*, 8207−8215.
(78) Heyd, J.; Scuseria, G. E. Efficient hybrid density functional calculations in solids: Assessment of the Heyd-Scuseria-Ernzerhof screened Coulomb hybrid functional. *J. Chem. Phys.* **2004**, *121*, 1187−1192.
(79) Henderson, T. M.; Izmaylov, A. F.; Scalmani, G.; Scuseria, G. E. Can short-range hybrids describe long-range-dependent properties? *J. Chem. Phys.* **2009**, *131*, No. 044108.
(80) Vydrov, O. A.; Scuseria, G. E. Assessment of a long-range corrected hybrid functional. *J. Chem. Phys.* **2006**, *125*, No. 234109.
(81) Zhao, Y.; Schultz, N. E.; Truhlar, D. G. Exchange-correlation functional with broad accuracy for metallic and nonmetallic compounds, kinetics, and noncovalent interactions. *J. Chem. Phys.* **2005**, *123*, No. 161103.
(82) Zhao, Y.; Schultz, N. E.; Truhlar, D. G. Design of density functionals by combining the method of constraint satisfaction with parametrization for thermochemistry, thermochemical kinetics, and noncovalent interactions. *J. Chem. Theory Comput.* **2006**, *2*, 364−382.
(83) Zhao, Y.; Truhlar, D. G. The M06 suite of density functionals for main group thermochemistry, thermochemical kinetics, noncovalent interactions, excited states, and transition elements: Two new functionals and systematic testing of four M06-class functionals and 12 other functionals. *Theor. Chem. Acc.* **2008**, *120*, 215−241.
(84) Zhao, Y.; Truhlar, D. G. Density functional for spectroscopy: No long-range self-interaction error, good performance for Rydberg and charge-transfer states, and better performance on average than B3LYP for ground states. *J. Phys. Chem. A* **2006**, *110*, 13126−13130.
(85) Peverati, R.; Truhlar, D. G. Improving the accuracy of hybrid meta-GGA density functionals by range separation. *J. Phys. Chem. Lett.* **2011**, *2*, 2810−2817.
(86) Peverati, R.; Truhlar, D. G. Screened-exchange density functionals with broad accuracy for chemistry and solid-state physics. *Phys. Chem. Chem. Phys.* **2012**, *14*, 16187−16191.
(87) Adamo, C.; Barone, V. Exchange functionals with improved long-range behavior and adiabatic connection methods without adjustable parameters: The mPW and mPW1PW models. *J. Chem. Phys.* **1998**, *108*, 664−675.
(88) Perdew, J. P.; Chevary, J. A.; Vosko, S. H.; Jackson, K. A.; Pederson, M. R.; Singh, D. J.; Fiolhais, C. Atoms, molecules, solids, and surfaces: Applications of the generalized gradient approximation for exchange and correlation. *Phys. Rev. B* **1992**, *46*, 6671−6687.
(89) Ernzerhof, M.; Perdew, J. P. Generalized gradient approximation to the angle- and system-averaged exchange hole. *J. Chem. Phys.* **1998**, *109*, 3313−3320.
(90) Peverati, R.; Truhlar, D. G. Communication: A global hybrid generalized gradient approximation to the exchange-correlation functional that satisfies the second-order density-gradient constraint and has broad applicability in chemistry. *J. Chem. Phys.* **2011**, *135*, No. 191102.
(91) Staroverov, V. N.; Scuseria, G. E.; Tao, J.; Perdew, J. P. Comparative assessment of a new nonempirical density functional: Molecules and hydrogen-bonded complexes. *J. Chem. Phys.* **2003**, *119*, 12129−12137.
(92) Xu, X.; Goddard, W. A., III The X3LYP extended density functional for accurate descriptions of nonbond interactions, spin states, and thermochemical properties. *Proc. Natl. Acad. Sci. U.S.A.* **2004**, *101*, 2673−2677.
(93) Schäfer, A.; Huber, C.; Ahlrichs, R. Fully optimized contracted Gaussian basis sets of triple zeta valence quality for atoms Li to Kr. *J. Chem. Phys.* **1994**, *100*, 5829−5835.
(94) Binkley, J. S.; Pople, J. A.; Hehre, W. J. Self-consistent molecular orbital methods. 21. Small split-valence basis sets for first-row elements. *J. Am. Chem. Soc.* **1980**, *102*, 939−947.
(95) Hehre, W. J.; Ditchfield, R.; Pople, J. A. Self-consistent molecular orbital methods. XII. Further extensions of Gaussian-type basis sets for use In molecular orbital studies of organic molecules. *J. Chem. Phys.* **1972**, *56*, 2257−2261.
(96) Schäfer, A.; Horn, H.; Ahlrichs, R. Fully optimized contracted Gaussian basis sets for atoms Li to Kr. *J. Chem. Phys.* **1992**, *97*, 2571−2577.
(97) Weigend, F.; Furche, F.; Ahlrichs, R. Gaussian basis sets of quadruple zeta valence quality for atoms H-Kr. *J. Chem. Phys.* **2003**, *119*, 12753−12762.
(98) Weigend, F.; Ahlrichs, R. Balanced basis sets of split valence, triple zeta valence and quadruple zeta valence quality for H to Rn: Design and assessment of accuracy. *Phys. Chem. Chem. Phys.* **2005**, *7*, 3297−3305.
(99) Jensen, F. Polarization consistent basis sets: Principles. *J. Chem. Phys.* **2001**, *115*, 9113−9125.
(100) Korth, M.; Grimme, S. "Mindless" DFT Benchmarking. *J. Chem. Theory Comput.* **2009**, *5*, 993−1003.
(101) Lee, T. J.; Bauschlicher, C. W.; Dateo, C. E.; Rice, J. E. The molecular structure of cis-FONO. *Chem. Phys. Lett.* **1994**, *228*, 583−588.
(102) Lee, T. J.; Bauschlicher, C. W.; Jayatilaka, D. A challenge for density functional theory: The XONO and XNO_2 (X=F, Cl, and Br) molecules. *Theor. Chem. Acc.* **1997**, *97*, 185−194.
(103) Vacek, G.; Galbraith, J. M.; Yamaguchi, Y.; Schaefer, H. F., III; Nobes, R. H.; Scott, A. P.; Radom, L. Oxirene: To be or not to be. *J. Phys. Chem.* **1994**, *98*, 8660−8665.
(104) Simmie, J. M.; Somers, K. P. Benchmarking compound methods (CBS-QB3, CBS-APNO, G3, G4, W1BD) against the Active Thermochemical Tables: A litmus test for cost-effective molecular formation enthalpies. *J. Phys. Chem. A* **2015**, *119*, 7235−7246.
(105) Frisch, M. J.; Trucks, G. W.; Schlegel, H. B.; Scuseria, G. E.; Robb, M. A.; Cheeseman, J. R.; Scalmani, G.; Barone, V.; Mennucci, B.; Petersson, G. A. et al. *Gaussian 09*, revision A.02; Gaussian, Inc.: Wallingford, CT.
(106) Moran, D.; Simmonett, A. C.; Leach, F. E., III; Allen, W. D.; Schleyer, P. vR.; Schaefer, H. F., III Popular theoretical methods predict benzene and arenes to be nonplanar. *J. Am. Chem. Soc.* **2006**, *128*, 9342−9343.
(107) Purvis, G. D.; Bartlett, R. J. A full coupled-cluster singles and doubles model: The inclusion of disconnected triples. *J. Chem. Phys.* **1982**, *76*, 1910−1918.
(108) Raghavachari, K.; Trucks, G. W.; Pople, J. A.; Head-Gordon, M. A fifth-order perturbation comparison of electron correlation theories. *Chem. Phys. Lett.* **1989**, *157*, 479−483.
(109) Hampel, C.; Peterson, K. A.; Werner, H.-J. A comparison of the efficiency and accuracy of the quadratic configuration interaction (QCISD), coupled cluster (CCSD), and Brueckner coupled cluster (BCCSD) methods. *Chem. Phys. Lett.* **1992**, *190*, 1−12.
(110) Stanton, J. F.; Gauss, J.; Cheng, L.; Harding, M. E.; Matthews, D. A.; Szalay, P. G. CFOUR, Coupled-Cluster Techniques for Computational Chemistry, a Quantum-Chemical Program Package with contributions from A.A. Auer, R.J. Bartlett, U. Benedikt, C. Berger, D.E. Bernholdt, Y.J. Bomble, O. Christiansen, F. Engel, R. Faber, M. Heckert, O. Heun, M. Hilgenberg, C. Huber, T.-C. Jagau, D. Jonsson, J. Jusélius, T. Kirsch, K. Klein, W.J. Lauderdale, F. Lipparini, T. Metzroth, L.A. Mück, D.P. O'Neill, D.R. Price, E. Prochnow, C. Puzzarini, K. Ruud, F. Schiffmann, W. Schwalbach, C. Simmons, S. Stopkowicz, A. Tajti, J. Vázquez, F. Wang, J.D. Watts and the integral packages MOLECULE (J. Almlöf and P.R. Taylor), PROPS (P.R. Taylor), ABACUS (T. Helgaker, H.J. Aa. Jensen, P. Jørgensen, and J. Olsen), and ECP routines by A. V. Mitin and C. van Wüllen. For the current version, see http://www.cfour.de.
(111) Some of the basis sets were obtained from the EMSL basis set library, see refs 112 and 113.
(112) Feller, D. The role of databases in support of computational chemistry calculations. *J. Comput. Chem.* **1996**, *17*, 1571−1586.
(113) Schuchardt, K. L.; Didier, B. T.; Elsethagen, T.; Sun, L.; Gurumoorthi, V.; Chase, J.; Li, J.; Windus, T. L. Basis set exchange: A community database for computational sciences. *J. Chem. Inf. Model.* **2007**, *47*, 1045−1052.
(114) Peterson, K. A.; Woon, D. E.; Dunning, T. H., Jr. Benchmark calculations with correlated molecular wave functions. IV. The

https://doi.org/10.1021/acs.jctc.1c00474
J. Chem. Theory Comput. 2021, 17, 4872−4890

classical barrier height of the H+H_2->H_2+H reaction. *J. Chem. Phys.* **1994**, *100*, 7410−7415.
(115) Woon, D. E.; Dunning, T. H., Jr. Gaussian basis sets for use in correlated molecular calculations. V. Core-valence basis sets for boron through neon. *J. Chem. Phys.* **1995**, *103*, 4572−4585.
(116) Werner, H.-J.; Knowles, P. J.; Knizia, G.; Manby, F. R.; Schütz, M.; Celani, P.; Györffy, W.; Kats, D.; Korona, T.; Lindh, R.; Mitrushenkov, A.; Rauhut, G.; Shamasundar, K. R.; Adler, T. B.; Amos, R. D.; Bernhardsson, A.; Berning, A.; Cooper, D. L.; Deegan, M. J. O.; Dobbyn, A. J.; Eckert, F.; Goll, E.; Hampel, C.; Hesselmann, A.; Hetzer, G.; Hrenar, T.; Jansen, G.; Köppl, C.; Liu, Y.; Lloyd, A. W.; Mata, R. A.; May, A. J.; McNicholas, S. J.; Meyer, W.; Mura, M. E.; Nicklass, A.; O'Neill, D. P.; Palmieri, P.; Peng, D.; Pflüger, K.; Pitzer, R.; Reiher, M.; Shiozaki, T.; Stoll, H.; Stone, A. J.; Tarroni, R.; Thorsteinsson, T.; Wang, M. MOLPRO, Version 2015.1: A Package of Ab Initio Programs, 2015. See http://www.molpro.net. (Earlier versions 2006.1 and 2012.1 have been used as well).
(117) Werner, H.-J.; Knowles, P. J.; Knizia, G.; Manby, F. R.; Schütz, M. Molpro: A general-purpose quantum chemistry program package. *Wiley Interdiscip. Rev.: Comput. Mol. Sci.* **2012**, *2*, 242−253.
(118) Ahlrichs, R.; Bär, M.; Häser, M.; Horn, H.; Kölmel, C. Electronic structure calculations on workstation computers: The program system TURBOMOLE. *Chem. Phys. Lett.* **1989**, *162*, 165−169.
(119) TURBOMOLE, A Development of University of Karlsruhe and Forschungszentrum Karlsruhe GmbH, 1989−2007, TURBOMOLE GmbH, since 2007. Available from http://www.turbomole.com.
(120) Weigend, F.; Häser, M.; Patzelt, H.; Ahlrichs, R. RI-MP2: Optimized auxiliary basis sets and demonstration of efficiency. *Chem. Phys. Lett.* **1998**, *294*, 143−152.
(121) Weigend, F.; Köhn, A.; Hättig, C. Efficient use of the correlation consistent basis sets in resolution of the identity MP2 calculations. *J. Chem. Phys.* **2002**, *116*, 3175−3183.
(122) Hättig, C. Optimization of auxiliary basis sets for RI-MP2 and RI-CC2 calculations: Core-valence and quintuple-zeta basis sets for H to Ar and QZVPP basis sets for Li to Kr. *Phys. Chem. Chem. Phys.* **2005**, *7*, 59−66.
(123) Stanton, J. F.; Gauss, J.; Cheng, L.; Harding, M. E.; Matthews, D. A.; Szalay, P. G. CFOUR, Coupled-Cluster Techniques for Computational Chemistry, a Quantum-Chemical Program Package, version 1.0. 2010, For the current version, see http://www.cfour.de.
(124) Spackman, P. R.; Jayatilaka, D.; Karton, A. Basis set convergence of CCSD(T) equilibrium geometries using a large and diverse set of molecular structures. *J. Chem. Phys.* **2016**, *145*, No. 104101.
(125) Warden, C. E.; Smith, D. G. A.; Burns, L. A.; Bozkaya, U.; Sherrill, C. D. Efficient and automated computation of accurate molecular geometries using focal-point approximations to large-basis coupled-cluster theory. *J. Chem. Phys.* **2020**, *152*, No. 124109.
(126) Curtiss, L. A.; Redfern, P. C.; Raghavachari, K.; Pople, J. A. Gaussian-3X (G3X) theory: Use of improved geometries, zero-point energies, and Hartree-Fock basis sets. *J. Chem. Phys.* **2001**, *114*, 108−117.
(127) Peterson, C.; Penchoff, D. A.; Wilson, A. K. Prediction of thermochemical properties across the periodic table: A review of the correlation consistent composite approach (ccCA) strategies and applications. *Annu. Rep. Comput. Chem.* **2016**, *12*, 3−45.
(128) Pople, J. A.; Scott, A. P.; Wong, M. W.; Radom, L. Scaling factors for obtaining fundamental vibrational frequencies and zero-point energies from HF/6-31G* and MP2/6-31G* harmonic frequencies. *Isr. J. Chem.* **1993**, *33*, 345−350.
(129) Scott, A. P.; Radom, L. Harmonic vibrational frequencies: An evaluation of Hartree-Fock, Møller-Plesset, quadratic configuration interaction, density functional theory, and semiempirical scale factors. *J. Phys. Chem.* **1996**, *100*, 16502−16513.
(130) Merrick, J. P.; Moran, D.; Radom, L. An evaluation of harmonic vibrational frequency scale factors. *J. Phys. Chem. A* **2007**, *111*, 11683−11700.
(131) Kesharwani, M. K.; Brauer, B.; Martin, J. M. L. Frequency and zero-point vibrational energy scale factors for double-hybrid density functionals (and other selected methods): Can anharmonic force fields be avoided? *J. Phys. Chem. A* **2015**, *119*, 1701−1714.
(132) Karton, A.; Yu, L.-J.; Kesharwani, M. K.; Martin, J. M. L. Heats of formation of the amino acids re-examined by means of W1-F12 and W2-F12 theories. *Theor. Chem. Acc.* **2014**, *133*, No. 1483.
(133) Chan, B.; Radom, L. Frequency scale factors for some double-hybrid density functional theory procedures: Accurate thermochemical components for high-level composite protocols. *J. Chem. Theory Comput.* **2016**, *12*, 3774−3780.
(134) Grimme, S. Semiempirical hybrid density functional with perturbative second-order correlation. *J. Chem. Phys.* **2006**, *124*, No. 034108.
(135) Schwabe, T.; Grimme, S. Towards chemical accuracy for the thermodynamics of large molecules: New hybrid density functionals including non-local correlation effects. *Phys. Chem. Chem. Phys.* **2006**, *8*, 4398−4401.
(136) Berski, S.; Latajka, Z.; Gordon, A. J. Quantum chemical topology study on the electronic structure of cis- and trans-FONO. *J. Chem. Phys.* **2010**, *133*, No. 034304.
(137) Beachy, M. D.; Chasman, D.; Murphy, R. B.; Halgren, T. A.; Friesner, R. A. Accurate ab initio quantum chemical determination of the relative energetics of peptide conformations and assessment of empirical force fields. *J. Am. Chem. Soc.* **1997**, *119*, 5908−5920.
(138) Alanine tetrapeptide continues to be a popular benchmark system to assess the accuracy of approximate methods in reproducing high-level conformational energies for given sets of geometries. The study of Kang and Park (ref 139) is a recent example which also reviews other work that has appeared since the original publication of Beachy et al. (ref 137).
(139) Kang, Y. K.; Park, H. S. Exploring conformational preferences of alanine tetrapeptide by CCSD(T), MP2, and dispersion-corrected DFT methods. *Chem. Phys. Lett.* **2018**, *702*, 69−75.
(140) Distasio, R. A.; Steele, R. P.; Rhee, Y. M.; Shao, Y.; Head-Gordon, M. An improved algorithm for analytical gradient evaluation in resolution-of-the-identity second-order Møller-Plesset perturbation theory: Application to alanine tetrapeptide conformational analysis. *J. Comput. Chem.* **2007**, *28*, 839−856.
(141) Scott, A. P.; Nobes, R. H.; Schaefer, H. F., III; Radom, L. The Wolff rearrangement: The relevant portion of the oxirene-ketene potential energy hypersurface. *J. Am. Chem. Soc.* **1994**, *116*, 10159−10164.
(142) Guan, J.; Randall, K. R.; Schaefer, H. F., III; Li, H. Formylmethylene: The triplet ground state and the lowest singlet state. *J. Phys. Chem. A* **2013**, *117*, 2152−2159.
(143) Feller, D.; Dixon, D. A. Coupled cluster theory and multireference configuration interaction study of FO, F_2O, FO_2, and FOOF. *J. Phys. Chem. A* **2003**, *107*, 9641−9651.
(144) Karton, A.; Parthiban, S.; Martin, J. M. L. Post-CCSD(T) ab initio thermochemistry of halogen oxides and related hydrides XOX, XOOX, HOX, XO_n, and HXO_n, (X = F, Cl), and evaluation of DFT methods for these systems. *J. Phys. Chem. A* **2009**, *113*, 4802−4816.
(145) Cases with imaginary frequencies reported in Table S1 have been resolved for this comparison. See footnate a of Table S6.
(146) Csonka, G. I.; Ruzsinszky, A.; Perdew, J. P. Estimation, computation, and experimental correction of molecular zero-point vibrational energies. *J. Phys. Chem. A* **2005**, *109*, 6779−6789.
(147) Breidung, J.; Schneider, W.; Thiel, W.; Lee, T. J. The vibrational frequencies of difluoroethyne. *J. Chem. Phys.* **1992**, *97*, 3498−3499.
(148) Borro, A. F.; Mills, I. M.; Mose, A. Overtone spectra and anharmonic resonances in haloacetylenes. *Chem. Phys.* **1995**, *190*, 363−371.
(149) Jones, L. H. Force field of cyanogen from vibrational spectra of isotopic species. *J. Mol. Spectrosc.* **1974**, *49*, 82−90.
(150) Koops, T.; Visser, T.; Smit, W. M. A. The harmonic force field and absolute infrared intensities of diacetylene. *J. Mol. Struct.* **1984**, *125*, 179−196.

https://doi.org/10.1021/acs.jctc.1c00474
J. Chem. Theory Comput. 2021, 17, 4872−4890

(151) McNaughton, D.; Elmes, P. High resolution Fourier transform infrared spectrum of difluoroethyne, FCCF. *Spectrochim. Acta, Part A* **1992**, *48*, 605−611.
(152) Bernardes, E. S.; Hornos, Y. M. M.; Hornos, J. E. M. Dynamical symmetry in the vibrational overtone spectrum of monofluoroacetylene (HCCF). *Chem. Phys.* **1996**, *213*, 17−32.
(153) Shimanouchi, T. Tables of molecular vibrational frequencies. Consolidated volume II. *J. Phys. Chem. Ref. Data* **1977**, *6*, 993−1102.
(154) Irikura, K. K.; Johnson, R. D., III; Kacker, R. N.; Kessel, R. Uncertainties in scaling factors for ab initio vibrational zero-point energies. *J. Chem. Phys.* **2009**, *130*, No. 114102.
(155) Pernot, P.; Cailliez, F. Comment on "Uncertainties in scaling factors for ab initio vibrational zero-point energies" [J. Chem. Phys. 130, 114102 (2009)] and "Calibration sets and the accuracy of vibrational scaling factors: A case study with the X3LYP hybrid functional" [J. Chem. Phys. 133, 114109 (2010)]. *J. Chem. Phys.* **2011**, *134*, No. 167101.
(156) Irikura, K. K.; Johnson, R. D., III; Kacker, R. N.; Kessel, R. Response to "Comment on 'Uncertainties in scaling factors for ab initio vibrational zero-point energies' and 'Calibration sets and the accuracy of vibrational scaling factors: A case study with the X3LYP hybrid functional'" [J. Chem. Phys. 134, 167101 (2011)]. *J. Chem. Phys.* **2011**, *134*, No. 167102.

https://doi.org/10.1021/acs.jctc.1c00474
J. Chem. Theory Comput. 2021, 17, 4872−4890